sustainability

MDPI

Review

Review on Urban Heat Island in China: Methods, Its Impact on Buildings Energy Demand and Mitigation Strategies

Liu Tian, Yongcai Li *, Jun Lu and Jue Wang

Key Laboratory of Three Gorges Reservoir Region's Eco-Environment, Ministry of Education, Chongqing University, Chongqing 400045, China; 20151702048@cqu.edu.cn (L.T.); lujun@cqu.edu.cn (J.L.); 20145403@cqu.edu.cn (J.W.)

* Correspondence: yongcail85@163.com; Tel.: +86-(0)23-6512-3777

Abstract: High population density, dense high-rise buildings, and impervious pavements increase the vulnerability of cities, which aggravate the urban climate environment characterized by the urban heat island (UHI) effect. Cities in China provide unique information on the UHI phenomenon because they have experienced rapid urbanization and dramatic economic development, which have had a great influence on the climate in recent decades. This paper provides a review of recent research on the methods and impacts of UHI on building energy consumption, and the practical techniques that can be used to mitigate the adverse effects of UHI in China. The impact of UHI on building energy consumption depends largely on the local microclimate, the urban area features where the building is located, and the type and characteristics of the building. In the urban areas dominated by air conditioning, UHI could result in an approximately 10–16% increase in cooling energy consumption. Besides, the potential negative effects of UHI can be prevented from China in many ways, such as urban greening, cool material, water bodies, urban ventilation, etc. These strategies could have a substantial impact on the overall urban thermal environment if they can be used in the project design stage of urban planning and implemented on a large scale. Therefore, this study is useful to deepen the understanding of the physical mechanisms of UHI and provide practical approaches to fight the UHI for the urban planners, public health officials, and city decision-makers in China.

Keywords: urban heat island; building energy consumption; research method; mitigation strategies

Citation: Tian, L.; Li, Y.; Lu, J.; Wang, J. Review on Urban Heat Island in China: Methods, Its Impact on Buildings Energy Demand and Mitigation Strategies. *Sustainability* **2021**, *13*, 762. https://doi.org/10.3390/su13020762

Received: 6 December 2020
Accepted: 11 January 2021
Published: 14 January 2021

1. Introduction

As the main sites of human activities and interactions, cities are facing great changes in land use and land cover (LULC) due to population growth and economic development [1]. The natural land surfaces in cities, mainly vegetation and permeable areas, have been transformed into built-up and impervious areas [2]. According to the report released by the United Nations in 2014, the proportion of urban population around the world is growing rapidly, with 54% of the world's population moving to cities, and this fraction is expected to reach 66% by 2050 [3]. At the same time, urbanization has become a major concern of many countries worldwide because of its adverse impact on ecology and the environment; in particular, the urban heat island (UHI) effect is one of the significant environmental impacts of urbanization [4,5].

The UHI phenomena have had many adverse effects on the urban social ecosystem, including increasing building energy consumption, reducing thermal comfort, affecting the health of urban residents, and decreasing urban air quality [6–13]. Several studies have documented the specific effects of UHI on electricity demand and energy use for cooling. In Europe, data shows that when the temperature increases by 1 °C in summer, electricity consumption is increased by 1.66% in hot climatic countries and by 0.542% in mild climatic countries [14]. In the Mediterranean region, energy demands for cooling buildings increased by 12% in the peripheral neighborhood of the city and by 46% in the

city centers due to the UHI effect [15]. Li et al. [16] found that UHI can increase the median cooling energy consumption by 19.0%. In addition, the most immediate effect of UHI on human health is through exposure to rising temperatures, while higher temperatures increase the risk of human death during heat waves [17–19]. In the UK, a study showed that extreme urban overheating is expected to be exacerbated due to UHI phenomenon [20]. Therefore, many mitigation strategies have been proposed to reduce the risk of UHI, such as urban green spaces (UGS), green roofs (GR), vertical greening (VG), natural water bodies, cool materials, and changing the urban geometry. [14,21–24].

The study of the UHI effect has drawn increasing attention to scholars all over the world. Many review articles related to the UHI phenomenon have been published in the last decade. Most of these studies have focused on the mitigation measures for the UHI, and the effect of UHI on building energy consumption and outdoor thermal comfort. The research region of these articles is usually for the whole world, and few UHI related articles focus on specific regions. China is an ideal case to investigate the UHI effect, given that it has experienced the most rapid urbanization in the past decades and this trend is expected to continue in the coming decades [25,26]. Therefore, more research is needed in China to better understand the UHI effect and to provide guidance for appropriate policies-making and planning to mitigate the UHI effect.

In order to review and analyze the available scientific information on UHI studies in China, a literature survey was conducted in this paper. Related UHI papers were retrieved in two comprehensive databases: Science Direct and Web of Science. The search was limited to the year 2010–2019. Several generic phrases, such as "urban heat island" and "heat island", were used to query titles, keywords, and abstracts in both databases. The selected papers were published in international peer-reviewed journals or proceedings of international conferences. Based on this, articles unrelated to the impact of UHI on building energy consumption and UHI mitigation strategies in China were filtered out. This filtering phase is based on the full text of the retrieved papers.

The structure of this review is as follows: the concept and formation of UHI are introduced in Section 2, followed by summarizing the different methods to study UHI in Section 3. Section 4 discusses the UHI status and its impact on building energy consumption in China. The strategies for mitigating the UHI effect in China, including UGS, GR, VG, urban morphology, cool material, water bodies, and urban ventilation are summarized in Section 5. Finally, we discuss the mitigation effects of the strategies and the effectiveness of these strategies in mitigating the UHI phenomenon. These findings will guide the planning and management of Chinese UHI areas and promote the conservation and sustainable use of natural sources in Chinese cities to increase urban environmental benefits and mitigate the impact of high temperatures in urban areas.

2. Generic Viewpoints on UHI

2.1. Concepts of UHI, UHII and UCI

Urban regions absorb more solar radiation and have a great thermal capacity due to the massive buildings, pavements, and other surfaces [27,28]. They are likely to suffer from higher temperatures than the suburban and rural areas. The UHI phenomenon, which is closely related to climate change and urban development, generally describes the excess warmth of the urban areas in comparison to the neighboring suburban and rural areas [29–32]. The term of UHI was first established by Howard in 1820 when he discovered the temperature difference between night and day in London compared to the surroundings [33]. It was defined by Oke and Voogt in terms of various layers of the urban atmosphere, various surfaces, and even subsurface [34,35].

UHI is currently divided into boundary layer UHI (BLUHI), canopy layer UHI (CLUHI), and surface UHI (SUHI) due to different research scopes [36–38]. BLUHI is measured from building roof to the atmosphere, CLUHI is measured from the ground to building roof, and SUHI is measured from the ground [36,39,40]. BLUHI is generally used to investigate the UHI effect on mesoscale, collected by weather towers, aircraft, or

satellites [38]. CLUHI is suitable for microscale studies, derived by stationary sites or mobile transverse methods [41,42]. SUHI can be obtained using satellite thermal images to invert land surface temperature (LST) [38]. At present, most studies focus on the UHI characteristics of urban surface and urban canopy. The temperature records of meteorological measurements can well indicate the interannual, seasonal, or diurnal variations of UHI, but uneven time series of temperature records often leads to uncertainty of the warming trend [43]. Using satellite images can rapidly evaluate vast geographic regions and can provide detailed information on the surface temperature changes of different land cover types [44–46]. However, it has pixel size and validation limitations, which are not ideal for evaluating microscale areas.

The magnitude of UHI can be expressed in terms of urban heat island intensity (UHII), which is the temperature difference between urban areas and rural ones [47]. It is an important indicator when evaluating the severity of the UHI effect or urbanization [48].

Urban cool island (UCI) phenomenon, known as the negative heat island, refers to the fact that the temperature of a certain area of the city is lower than the average temperature of the surrounding area [49,50]. It can be observed from the urban green spaces, urban wetlands (including reservoirs, lakes, and rivers), and the shade of high-rise buildings or the light-colored materials [51–54]. Compared to UHI, UCI is particularly prone to occur in the morning or noon periods because of the strong urban thermal turbulent exchange at the time, and the intensity of UCI is usually weaker than UHI [36,55].

2.2. UHI Contributing Factors

The urban texture is different from that of nature, solar radiation and anthropogenic heat are the primary thermal sources within a city. The surface energy balance (SEB) is helpful for the understanding of the UHI phenomenon [56]:

$$Q^* + Q_F = Q_H + Q_E + \Delta Q_S + \Delta Q_A \left(\mathrm{W/m^2}\right) \quad (1)$$

The fluxes Q^*, Q_F, Q_H, Q_E, ΔQ_S, and ΔQ_A in Equation (1) are net all-wave radiation, anthropogenic heat, sensible heat, latent heat, energy flux storage, and advection, respectively. Q_F is often ignored or proxy values are used due to the lack of appropriate data in cities. However, there is evidence that it could be significant especially in high-density cities depending on location and its energy use [57,58]. Many studies have reported that Q^* has the highest values during solar peak time, followed by Q_H, Q_E, and ΔQ_S [59,60]. Q_H and Q_E are the largest parts of daytime SEB in urban and rural areas, respectively. Conversely, ΔQ_S is the main heat output during night-time. In addition, ΔQ_A caused by the complex terrain can be ignored in the case that flux densities and scalars are distributed in horizontal and homogenous patterns [61].

UHI is caused by the positive energy balance in urban areas, and the magnitude and characteristics of UHI are influenced and determined by numerous parameters. Previous research has shown that UHI changes were negatively related to humidity, precipitation, wind speed, and cloud cover [62–65]. UHI is more intense in the anticyclonic regime [66]. As urbanization is progressing, the natural and semi-natural surfaces are transformed into impermeable urban structures, which disrupt the balance of SEB and the composition of near-surface atmospheric structures [67]. This often results in a decrease in evaporating surfaces, low sky view factors (SVF), and increase of atmospheric pollution in the urban environment [68,69]. Therefore, the urban temperature will increase due to the absorption and storage of solar radiation on complicated urban surfaces, the reduction of SVF, and the decrease of thermal inertia and vegetation index [70–73]. The emission of infrared radiation from pollutants can increase the thermal balance of the urban environment [6]. In addition, urban anthropogenic activity is also an important factor to induce UHI [74,75].

3. Methods of Studying UHI

Generally, a variety of approaches are employed to assess UHI such as meteorological observation, fixed measurements or mobile traverse methods, remote sensing, and numerical simulation [76–78]. In this section, a comprehensive review of research approaches for UHI over the past decade is presented.

3.1. Meteorological Observation

Meteorological observation methods refer to studying the variability of UHI (monthly, seasonal, inter-annual, and inter-decadal) using long-term meteorological data from both pre- and post-urbanization periods or urban and suburban (or rural) meteorological data in the same period [74,79]. UHI has an additive effect on long-term temperature trends [80]. To understand the impacts of UHI on different urban development and the temporal variability of UHII over long periods, it is demanded to assess UHI based on long-term monitoring data in urban areas [67,74]. Hong et al. [67] pointed out that long-term meteorological data is necessary as it appropriately describes the long-term trends of UHII.

Although a few studies focus on the meteorological data over long periods in China, recent studies have revealed that the observed climate change and surface warming in Eastern China (1961–2007) were induced by urbanization, with 44% of the warming in large cities due to the UHI effect [81]. Sun et al. [82] found that urban warming accounting for about a third of the observed warming between 1961 and 2013. Jiang et al. [83] found that the warming rate at urban meteorological stations was about three times greater than the average warming rate. Considering the special terrain conditions and the special local atmospheric circulation in the mountains or valley basins cities of China, the annual increase rate of UHII is +0.24 °C/decade in Lanzhou (1958–2015, valley city) and +0.10 °C/decade in Chongqing (1951–2010, mountain city) [84,85]. In addition, the relationships between the UHII and several factors of urban socioeconomic development, such as GDP level, industrial structures, and population size, were also analyzed by using meteorological data [85,86].

In general, the meteorological data can be used to study the UHI phenomenon in a city over a long period. It is noteworthy that the use of standard meteorological stations does not provide specific information on the microclimate [67,87]. The reference meteorological station to study the variability of UHII should be chosen carefully since many rural or suburban stations have experienced urbanization over time [74].

3.2. Fixed Measurements or Mobile Traverse Methods

Fixed measurements or mobile traverse methods refer to the use of portable mini-weather station or mobile traverses focus on the short-term data to assess UHI [74]. It provides the advantage of directly collecting the micro-climatic parameters (temperature, wind speed, solar radiation and relative humidity, etc.) [74,88]. The surveys are conducted on clear sunny days with the calm wind to avoid wind or rain affecting the measurement results. Fixed measurements are usually used to study the daily temperature variation, the influence of architectural elements on UHI reduction, and the thermal comfort in outdoor urban spaces [89–93]. However, when using fixed measurements, these data are limited in time and space. They are often combined with mobile survey or numerical simulation to provide the theoretical understanding and valuable information in urban thermal environment studies. Mobile traverse measurements, installing the instrumentations on a vehicle and running through the territory from the rural or suburb to the urban zone in order to measure data continuously, can give a full picture of the spatial distribution of temperature in detail and the local UHII along the mobile route [74,84,94]. However, it is difficult to get the spatial distribution of temperature in all urban areas due to the limited spatial coverage of the traverses and relatively few measurement parameters [26].

In China, in-situ measurements or mobile traverse methods are generally used to study microclimate regulation of the urban spaces on regional thermal environment, or the measured results are taken as the boundary conditions of simulation [95–97]. Many

researchers have also used this measurement method to study dynamic variations in UHII [86,87,98]. Furthermore, the integration of the measurement methods and spatial interpolation methods based on GIS is applied to obtain the spatial distributions of local UHII [94].

3.3. Remote Sensing Methods

Satellite remote sensing technology enables UHI research on a global scale and is open access, which has the potential to improve understanding of the UHI phenomenon and its effects [99,100]. The remote sensing research of UHI is carried out by using satellite-based thermal images, the satellite data usually used are MODIS (1 km), ASTER (90 m), Landsat-5-TM (120 m), Landsat-7-ETM+ (60 m), and Landsat-8-OLI/TIRS (100 m) [70,101]. Among them, more researchers use the MODIS and Landsat TM/ETM+/OLI data to study the UHI given open access to data acquisition and the spatial coverage of the study area. Thermal infrared bands have become one of the important means to study the UHI because the thermal channels of remote sensing data in the spectral region 10.4–12.5 μm of EMR spectrum have proven their capability to identify and evaluate UHI, while the most widely available thermal infrared bands come from Landsat TM/ETM+/OLI [102]. Currently, the mono-window algorithm and single-channel algorithm are well-developed algorithms for the retrieval of land surface temperature (LST) from Landsat TM/ETM+/OLI data [103]. In addition, MODIS LST data with high temporal resolution (twice daily temporal resolution) and wide coverage have been used to study the spatial, diurnal, and seasonal variations of UHI around the world in recent years [102,104]. Using remote sensing images to study the impacts of LULC on LST has been reported in a lot of literature about UHI [1,66,105,106]. Other vegetation and LULC indicators, such as normalized difference vegetation index (NDVI), normalized difference building index (NDBI), and impervious surface area ratio (ISAR), are also commonly retrieved and used for UHI estimation [107]. In addition, in order to get rid of the limitation of urban/rural divisions, a new approach to quantify UHII using the linear relationship between MODIS LST and impervious surface areas (ISA) was proposed by Li et al. [108]. On the whole, satellite-based thermal data are effective means to describe the spatial pattern of the urban thermal environment due to the characteristics of good spatial coverage and open and easy access. However, there are some limitations of this method, such as low temporal resolution, and the fact that the satellite may be affected by the cloud when it images over a specific land, and that the vertical temperature distributions cannot be captured [93,106,109].

A variety of studies using the remote sensing method have evaluated UHI in China. Research works related to UHI based on remote sensing methods in China are shown in Table 1. The proportion of studies using remote sensing technology to study UHI from different research areas in China is shown in Figure 1. According to the reviewed studies using remote sensing methods, in China, the UHII variations at different time scales, the cooling effects of green spaces or water body, the relationship between LULC and LST, and the characteristics of the UHI spatial patterns are the most studied topics in the last decade. The relation between the driving forces of urban development and UHI, and the impact of urban morphology (including SVF, building density, and floor area ratio, etc.) on LST has been mentioned in some studies. In these studies, cities of eastern China that have experienced rapid development in recent decades, such as, Beijing (23%), Shanghai (11%), Nanjing (5%), Hangzhou (7%), Guangzhou (5%), and Shenzhen (4%) are the most studied areas (see Figure 1). Furthermore, the study area of UHI is not always limited to a single city, but also includes urban agglomeration (including the Yangtze River Delta Urban Agglomeration, Beijing-Tianjin-Hebei Metropolitan Region, the Pearl-River-Delta Metropolitan Region, etc.; 11%), and even the whole of China (18%) (see Figure 1).

Table 1. Research related to urban heat island (UHI)-based on remote sensing methods in China.

Research Topics	Satellite Type	References
UHII variations (diurnal, seasonal and interannual)	Landsat TM/ETM+; MODIS	Ye et al. [110]; Qiao et al. [70]; Zhou et al. [25]; Huang et al. [111]; Li et al. [108]; Sheng et al. [112]; Yao et al. [113]; Yao et al. [114]; Lai et al. [46]; Yue et al. [115]; Zhou et al. [116]; Hu et al. [64]; Liu et al. [117]; Sun et al. [24]
UHI spatial patterns	Landsat TM/ETM+; MODIS	Zhang et al. [118]; Zhou [116]; Zhou et al. [26]; Meng et al. [119]; Lin et al. [120]; Liu et al. [117]; Peng et al. [86]; Yu et al. [121]
Cooling effects of UCI	ASTER; IKONOS; Landsat-8-OLI/TIRS; QuickBird	Sun et al. [51]; Kong et al. [122]; Du et al. [123]; Sun and Chen [124]; Cai et al. [125]; Wang et al. [126]; Yu et al. [121]
LULC and UHI	Landsat TM/ETM+; MODIS; HJ-1B; Landsat-8-TIRS; DMSP/OLS	Li et al. [127]; Zhang et al. [118]; Wu et al. [128]; Du et al. [129]; Wang [109]; Xu et al. [130]; Dai et al. [131]; Min et al. [78]; Wang et al. [126]; Yue et al. [115]; Yu et al. [132]
Related factors of urban development and UHI	Landsat TM/ETM+; MODIS	Chen et al. [133]; Yao et al. [114]; Zhou et al. [116]
Urban morphology and UHI	Landsat TM/ETM+/OLI; MODIS	Guo et al. [134]; Yue et al. [135]
Regional thermal environments of urban agglomerations	MODIS	Du et al. [129]; Wang et al. [109]; Zhou et al. [136]; Li et al. [137]; Sun et al. [5]; Yu et al. [121]; Yu et al. [132]
Building characteristics and anthropogenic heat release	MODIS	Cao et al. [75]

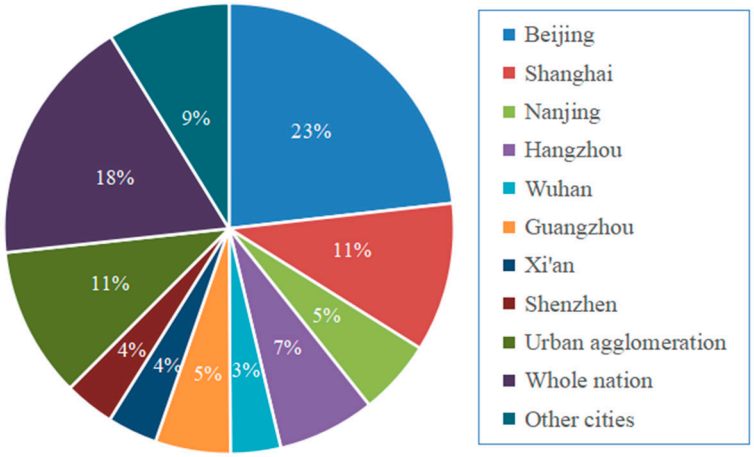

Figure 1. The proportion of studies using remote sensing methods to study UHI in different research areas (China), 56 references were included.

3.4. Numerical Simulation Methods

Numerical simulation is a method for predicting different environmental parameters (e.g., temperature, humidity, and speed) in urban space [138]. The measurement data of air or surface temperature are often used as boundary conditions in numerical simulation calculations, the results of which are compared with the measured data for analysis and optimization [91]. The numerical weather prediction (NWP) models ENVI-met, the computational fluid dynamics (CFD), urban canopy models (UCMs), building energy models (BEM), and statistical models are commonly used simulation tools to study the UHI at different spatial scales [139].

The characteristics of different simulation tools to study UHI are shown in Table 2. Numerical approaches at mesoscale are termed as NWP modes, covering a range within horizontal distances from a few to several hundred kilometers [140]. NWP models can be operated in a horizontal resolution of less than 1 km if the computational capacity is available. Several types of research studies use UCMs embedded within the NWP models to consider multi-reflections between urban surfaces, such as the coupled WRF/UCM mode at 300 m resolution [141–143]. The creation of numerical micro-scale models depends on the complex interactions between the urban fabric and local weather parameters, of which the widely employed simulation tools are UCMs, ENVI-met, and CFD [144]. The UCMs can predict the air temperature and surface temperature of buildings, roads, and pavements [145]. Although the calculation speed of UCM is fast, as it approximates the building with limited nodes, the main limitation of the model is the exclusion of the velocity field [71]. However, considering that wind velocities inside urban canyons can change the heat transfer in the local environment, it has a great impact on the UHI effect [71]. ENVI-met is a microclimate simulation tool that is used to assess microclimate to local climate scale environments, and it usually uses simplified numerical models with relatively low spatial resolution [146,147]. CFD simulations can be employed to study urban microclimate at different spatial scales, ranging from the microscale to the building scale and even the indoor environment [140,148]. In addition, combined with the solar radiation model, CFD can guarantee accuracy and efficiency in simulating temperature and relative humidity [130]. BEM is developed by the energy balance, which is mainly limited to individual buildings or isolated building envelope [27]. BEM models are usually integrated with other scale models to study the effect of UHI on building energy performance, for example. The town energy balance model (TEB) combines BEM models to predict the energy consumption of buildings and thermal conditions in urban canyons [27,60]. In addition, several studies have investigated the possibility of coupling CFD and BEM models [149,150].

Table 2. Overviews of different numerical simulation methods to study UHI.

Tools or Model	Scales ⋆	Type of Study UHI	Characteristics	Limitations	References
NWP models (MM5, WRF etc.)	Mesoscale	BLUHI	Large area coverage. Works for mesoscale phenomena.	Coarse resolution.	Wong et al. [151]; Touchaei et al. [152]; Souza et al. [153]; Liu et al. [142]; Morini et al. [141]; Takebayashi et al. [154]; Li et al. [77]
UCMs (such as TEB, BRAMS model)	Microscale	CLUHI	Reproduce the SEB, canyon air temperature and surface temperature.	Over-simplify the models of fluid flow and convective heat transfer.Weak in detail presentation of airflow around the buildings.	Mirzaei et al. [27]; Zeng and Gao [60]
ENVI-met	Microscale	CLUHI, SUHI	Have the ability to calculate the microclimatic dynamics of complex urban structures and calculate flow around and between buildings and heat exchange processes between the various surfaces.	The simplification of building facades to a single, averaged heat transfer coefficient. The lack of horizontal soil transfer within the model that potentially affects accurate calculations of soil heat storage. The applied turbulence models tending to overestimate the turbulent production in high acceleration area.	Taleb et al. [155]; Taleghani et al. [156]; Noro et al. [157]; O'Malley et al. [158]; Peron et al. [159]; Lin et al. [160]; Wang et al. [161]; Lu et al. [162]; Herath et al. [163]; Berardi et al. [164]
CFD (ANSYS Fluent/CFX, OpenFOAM, PHOENICS etc.)	Microscale, Building scale, Indoor environment	CLUHI, SUHI	Can explicitly resolve complicated urban land-atmosphere interactions. High spatial flow-field resolution can be obtained in regions of interest.	Simplifications to the urban geometry have to be made. Limited domain sizes due to the extensive computational cost. The accuracy of simulation results relies heavily on the boundary and initial condition settings.	Wong et al. [151]; Mirzaei et al. [27]; Heidarinejad et al. [165]; Allegrini et al. [149]; Yang et al. [166]
BEM (EnergyPlus, DOE2, eQUEST, ESP-r, TRNSYS, IESVirtual Environment)	Building scale, Indoor environment	SUHI	Widely employed in individual buildings or isolated building envelopes.	Models are simplistic in representing the mutual impact on a building with its surrounding area.	Kolokotsa et al. [167]; Rajagopalan et al. [168]; Martin et al. [169]; Mirzaei et al. [27]
Statistical models (ANN model, Regression methods)	Microscale, Building scale	CLUHI	Widely implemented to correlate the complex and large-scale characteristic of a city to the UHI.	Validated for a particular location and inapplicable to other regions. Results depend on available data due to the data-driven process.	Gobakis et al. [170]; Mirzaei et al. [27]; Lee et al. [171]; Parsaee et al. [172]
Urban porous media model	Microscale	CLUHI	Represent the macroscopic dynamic and thermodynamic effects of the building cluster on the urban airflow.	Incapable of demonstrating the detailed microscopic characteristics of the flow and temperature fields around individual building.	Hu et al. [173]
MITRAS	Mesoscale, Microscale	CLUHI	In addition to wind, temperature, humidity and tracer concentrations also equations for cloud- and rainwater and for chemical reactions are solved. Can be coupled with mesoscale models to account for the large-scale phenomena in microclimate simulations.	Have a rather low typical spatial resolution of a few meters.	Schlünzen et al. [174]; Allegrini et al. [148]

⋆ Scales: mesoscale (<200 km), microscale (<2 km), building scale (<100 m) and indoor environment (<10 m) [140].

The complexity of the UHI phenomenon and the bulk of urban details increase the cost and computational time of the modeling approaches, which give the statistical methods the advantages of being simpler and faster in the prediction studies [170,171,175]. It is noticeable, however, that artificial neural network (ANN) prediction studies require vast amounts of data to train the neural networks and predict the phenomenon [175].

Compared to other methods of the UHI research, the advantage of simulation studies is the ability to provide comparative analyses based on different scenarios and can provide results for any relevant variable in the whole study domain [71,140]. Considering the scale and complexity of urban environments, the simulation models used in UHI studies must be simplified; for this reason, validation of the simulations is very important [71].

4. UHI Status and its Impact on Building Energy Consumption in China

4.1. UHI Status in China

China has a total land area of 9.6 million square kilometers, with a north-south span of about 5500 km and an east-west span of about 5000 km [176]. Given its vast size, there are five main climate types in China, which are characterized by a variety of climate types and a remarkable monsoon climate, including temperate continental climate, temperate monsoon climate, subtropical monsoon climate, tropical monsoon climate, and plateau mountain climate.

As the largest developing country in the world, China's urbanization rate is significantly faster than other developing countries, from 17.92% to 58.52% during the period from 1978 to 2017 and is expected to reach 80% by 2050 [177]. Between 2008 and 2030, China's urban population will increase by 300–450 million [178]. Rapid urbanization in China has brought huge profits to stakeholders and has also brought many problems to the environment, society, and governance [179]. As a result of China's rapid development, the energy consumption of China has also increased dramatically. According to statistics, building energy consumption currently accounts for 27.5% of China's total energy consumption and is expected to account for about 40% in the next 20 years [180].

UHI, as an indication of urbanization's influence on urban thermal environment, is gradually increasing in China. The extent of the areas affected by UHI is largely based on the process of urban sprawl. A summary of studies on UHI in China is given in Table 3. On the whole, the UHII varies across cities in China due to the different development levels and climatic conditions, and the UHII in the same city also varies due to the different calculation methods or measuring time. Hu et al. [64] found that the average annual SUHI is higher than CUHI by comparing the UHI variation of the three cities in eastern China (Beijing, Shanghai, and Guangzhou). Yao et al. [113] studies the temporal trends of SUHI in 31 major cities in China, found that the SUHII of southern cities on days of summer and winter is higher than northern cities, while the opposite occurred in nights of summer and winter, which was consistent with the results of Zhou et al. [116]. In addition, the values of the daytime SUHII and the nighttime SUHII for a city also depend largely on the geographical location and research cycle [116]. Whether the daytime SUHII is higher or lower than the nighttime SUHII for a city also depends largely on the geographical location and research cycle [116].

Table 3. A summary of studies on UHI in China.

City	UHI Type	Considered Different Altitude	Approach ⋆	UHII (°C)					
				Minimum	Maximum	Mean	Day Time	Night Time	Reference
Beijing	CLUHI	Yes	MDM		8				Cui et al. [181]
	SUHI		RSM			2.33 ± 0.18			Hu et al. [64]
	CLUHI	Yes	MDM			1.45 ± 0.54	1.58	3.01	Hu et al. [64]
Chongqing	CLUHI		FMMTM; NSM		2.5				Yao et al. [88]
Shenzhen	CLUHI		FMMTM	−1	3	0–2			Liu et al. [182]
	CLUHI		FMMTM	1.2–1.4	2.5–2.8				Wang et al. [95]
	CLUHI		MDM; FMMTM		3	−1 to +1.5			Liu et al. [94]
Shanghai	SUHI		RSM			1.3			Cui et al. [183]
	SUHI		RSM			2.23 ± 0.11			Hu et al. [64]
	CLUHI	Yes	MDM			0.93 ± 0.41	2.95	1.41	Hu et al. [64]
Hangzhou	BLUHI		NSM		1.6	0.74			Chen et al. [184]
Shenyang	SUHI		RSM		6.69				Yao et al. [113]
Guangzhou	SUHI		RSM			2.13 ± 0.21			Hu et al. [64]
	CLUHI	Yes	MDM			0.89 ± 0.58	2.6	1.82	Hu et al. [64]
Yangtze River Delta Urban Agglomeration	SUHI		RSM	0.53	0.84		0.98	0.5	Du et al. [129]
China's 31 major cities	SUHI		RSM			4.09			Yao et al. [113]
China's 32 major cities	SUHI		RSM				0.01–1.87	0.35–1.95	Zhou et al. [116]

⋆ Approach: MDM, FMMTM, RSM, and NSM are meteorological data methods, fixed measurements or mobile traverses methods, remote sensing methods and numerical simulation methods, respectively.

4.2. Impact of the UHI on Building Energy Consumption in China

Studies have shown that buildings account for about 47% of total primary energy consumption in Switzerland, 42% in Brazil, 40% in the USA, 39% in the UK, 25% in Japan, and 23% in Spain [185]. In China, building energy demands accounted for about 24.1% of the total national energy use in 1996, which reached 27.5% in 2001 and is expected to reach about 35% in 2020 [186]. The UHI effect is considered as one of the important driving factors of building energy consumption by increasing the space cooling demand and reducing the space heating demand [16,187]. As a consequence of the UHI effect, the increased urban temperature directly affects the cooling energy use for buildings by increased energy use and heat dissipation of air conditioners. Li et al. [16] reviewed the existing literature of UHI impacts on building energy consumption and found that UHI increased average cooling energy consumption by 19.0% at the regional and global levels.

The influence of the UHI effect on energy consumption is mainly concentrated in urban areas. Different climate zones have different needs for cooling or heating energy. Compared with rural areas, UHI in urban areas of Beijing increased cooling load by 11% and reduced heating load by 16% [181]. Similarly, the UHI effect has increased the air conditioning demand by about 10% in the urban areas of Hong Kong [188,189]. In addition, the influence of UHI on building energy consumption varies with building types. Studies in Nanjing, China have shown that in the same studied period, the cooling load of the office building increased by 4.0–7.1%, while that of apartment building increased 11.2–25.2% [166]. The influence of UHI on building energy consumption also varies between the urban center and the urban periphery. The results of Zhou et al. [190] show that the heating load indexes of the buildings located downtown are 1.5–5.0% less than those in the suburbs. The average heating energy consumption of the buildings located downtown decreases by 5.04% with the UHII increasing by 1.0 °C.

5. Review of UHI Mitigation Strategies in China

In this section, recent studies in China have been systematically reviewed, reflecting the inventory of possible strategies to mitigate the UHI effect. The main objective of various strategies is to reduce the energy consumption and mitigate the urban environmental temperature.

5.1. Urban Greening

Artificial urban land uses such as buildings and roads covered by impermeable surfaces can contribute to the UHI formation, including reducing evapotranspiration, increasing storage and transfer from sensible heat, and reducing airflow [191]. Urban greening can purify the air, coordinate the temperature, regulate the local climate, and improve the city's ecosystem [192]. A growing number of studies have assessed potential urban greening remedies to mitigate the human health consequences of accelerating urban temperatures [21,33]. These studies provide evidence that urban greening, such as UGS, GR, and VG may play a role in cooling the environment at least locally.

5.1.1. Urban Green Spaces

UGS (including urban parks, road, residence and workplace greenspace, etc.) is considered an appropriate method to decrease the ambient air temperature, mitigate air pollution, provide comfort to the nearby occupants, and reduce cooling energy consumption in summer [18,23,193]. UGS can form the UCI effect by effective landscape planning, which has a good effect on alleviating UHI [194]. Tan et al. [192] found that small parks with highly tree planting and green space with lower SVF significantly reduced air temperature and formed UCI within park boundaries. The cooling effects of parks extend some distance beyond their boundaries and this extent is influenced by the character of the area around the park [195,196]. Park cooling could extend almost 1.4 km beyond the park's border in the study of Yan et al. [195]. Chang et al. [196] found that the larger the park size was, the stronger the UCI effect was.

Moreover, some studies have explored the potential benefits of UGS on savings in cooling energy in urban areas. Studies in Hong Kong showed that at least 1900 kWh of energy can be saved every day in summer when UGS coverage is about 30% [93]. Studies in Nanjing indicated that during the daytime hot summer period, 1.3×10^4 kWh energy could be saved when considering the cooling benefits of UGS [197]. Zhang et al. [198] found that the cooling effect of UGS in Beijing can save 60% of the net cooling energy consumption, and it has a strong correlation with the regional structure types of the city. The cooling effects of UGS are mainly determined by vegetation species, canopy density, and size and shape of UGS [131]. The mitigation effect of different types of UGS on the UHI effect was investigated by Xiao et al. [199], who found that compared with large UGS, small UGS not only have no cooling and humidifying effect, but also have heat preservation phenomenon in some cases. The urban cool island intensity (UCII) of different types of green lands was ranked as wedge green land > radial green land > punctate green land > banding green land [200].

Vegetation in urban environments can greatly improve microclimates and mitigate the UHI effect by shading and evapotranspiration, among that shade reduces sunlight reaching the ground and transpiration cools the ambient environment, creating UCI around vegetation [198,201]. At present, some studies have concerned the impact of different urban vegetation on the cooling effect. Beni et al. [201] found that trees with dense vegetation on the ground have a higher cooling effect than single trees or grass by field measurement. Tong et al. [202] found by field measurement that in the winter, compared with the obvious cooling effect of trees in summer, the effect was negligible due to the loss of leaf area and evaporation. In addition, increased greening and tree planting in urban areas is recommended to improve outdoor thermal comfort, while avoiding narrow street canyons to mitigate the UHI effect at night [202].

5.1.2. Green Roofs

GR, also known as ecological roofs, living roofs, and roof gardens, have s great potential to influence the surrounding urban environment, given that roofs account for nearly 20–25% of the city's surface area [203]. In China, where the majority of buildings in some major cities such as Beijing Shanghai, Chongqing, and Hong Kong, are very densely concentrated, the implementation of GR might have the potential to increase urban greenery coverage, save energy, reduce noise and air pollution [204–206]. Although GR increases initial investment compared to traditional roofs, they mitigate the UHI effect in urban areas, considering that green vegetation can significantly alter albedo values and reduce heat transfer to buildings [207,208]. A sensitivity test by He et al. [209] indicates that better thermal performance can be achieved in both the summer and winter by increasing the thickness of substrates or adopting GR on non-insulated buildings. Using three case studies, Tam et al. [210] found that GR can reduce indoor temperatures on the top floor by up to 3.4 °C. He et al. [209] found that the cooling effect of GR is the strongest in summer and weakest in winter for the Shanghai area.

The impact of GR on UHI depends on solar reflectivity, plant transpiration, plant density foliage, etc. [211]. Cao et al. [212] found that the plants with higher transpiration rates had a better cooling effect. In addition, GR is classified into intensive green roofs (IGR) and extensive green roofs (EGR) based on the depth of substrate [205,207,213]. Substrate depth of IGR is normally greater than 20 cm and can support diverse plant communities dominated by trees or other woody species, while EGR generally has a relatively shallow and light-weighted soil layer than IGR. A study in Hong Kong showed that the installation of EGR and IGR with 60% green coverage in the community can reduce the air temperature nearby by about 0.65 °C and 1.45 °C, and the saving energy annually was estimated to be 3.4×10^7 kWh and 7.6×10^7 kWh, respectively [213]. Nonetheless, considering the demand for heavy loading, regular maintenance, and benefit–cost ratio, EGR is more attractive compared to IGR [205,207]. Peng et al. [213] found that more complex IGR did not necessarily provide a better cooling effect than EGR.

Recent studies of GR in China have identified the advantages of GR in energy saving and improving the quality of the thermal environment. Kokogiannakis et al. [208] studied the thermal performance of GR across eight large Chinese cities, and their results showed that all types of IGR can reduce heat and cold loads compared to traditional non-insulated roofing. A study applying GR in Beijing found that the maximum indoor temperature decreases by about 7.0 °C in the cooling season, and the minimum indoor temperature increases by about 6.0 °C in the heating season [204]. Gao et al. [214] found that the use of GR can reduce the air-conditioned room's energy consumption by 0.106 kWh/m^2 in Chongqing and the average power saving rate was 25.0%. The research performed by Tang et al. [215] in Shanghai showed a 14.7% reduction in cooling energy consumption through the use of GR. Li et al. [216] found that buildings with GR and VG in Ningbo had an 8.8% reduction in cooling load and a 1.85% reduction in heating load.

In addition, the leaf area index (LAI) is a significant factor in the cooling effect [217,218]. Zeng et al. [218] found that in cooling-dominated cities (Chongqing and Guangzhou), GR can better improve indoor comfort than the cool roof, and the increase of LAI can lead to the reduction of annual energy consumption and cooling energy consumption. In addition, the combination of GR and night ventilation is widely used in summer cooling as passive energy-saving technologies. Jiang et al. [219] discovered that the combination of GR and night ventilation can reduce cooling energy consumption by up to 24.6% in June, especially in Beijing. Ran et al. [220] found that the cooling effect of the combination of GR and night ventilation becomes more obvious in the way of the improvement of the external wall insulation of buildings.

5.1.3. Vertical Greenery

Recently, VG, also known as 'vertical greening system' (VGS), 'vertical garden', 'green wall', and 'bio wall', has become increasingly popular in urban greening because of its small size, high aesthetic value, and UHI mitigation capability [221–225]. These effects can further result in psychological wellbeing and acoustic protections, protection of building envelope, and provision of biodiversity [222,226]. Based on their construction characteristics, green facades and living walls are the most extensively used classification for VGS [222,223,227,228]. Green facades can be divided into three different systems: traditional green facade (direct green facade, DGF), double-skin green facade (DSGF), and Living walls system (LWS) [229,230]. LWS can be classified into two groups: continuous living walls system and modular living walls system [222,229,230].

The VG of the building envelope can reduce the wall temperature to save energy through intercepting solar radiation, heat insulation provided by vegetation and matrix, evapotranspiration cooling, and acting as a wind screen [226,231]. Several researchers studied the impacts of VGS on urban temperature reduction. Yin et al. [227] found that DGF can significantly reduce the surface temperature of the building facade by up to 4.67 °C, and the cooling effect of DGF is the most obvious at noon. Zhang et al. [232] found that VGF could reduce the operating temperature by 3.6 °C due to plant shading and transpiration cooling in a subtropical city (Guangzhou, Guangdong province). Research conducted in Hong Kong by Dahanayake et al. [233] showed that VGS can reduce the exterior wall surface temperature up to 26 °C on hot summer days, while VGS may however increase the heating demand of the building depending on the outdoor conditions and solar radiation in winter. Cheng et al. [221] found that the building envelope with a green facade reduced air-conditioning energy consumption, and the cooling effect was closely related to the plant coverage area and the moisture in the growing medium. Pan et al. [231] found that VGS installed on the wall can save 16% of the total power consumption. A study of applying DSGF to high-rise residential buildings showed that VGS can reduce 2651 $\times$ 10^6 kWh of electricity and 2200 $\times$ 10^6 kg of carbon dioxide emission per year (Wong and Baldwin, 2016). Chen et al. [234] performed three series of LWS experiments and discovered that LWS has a significant cooling effect on wall surface temperature and the indoor temperature and increases the radiation heat transfer between the wall and LWS or decreases the convection

heat transfer between the wall and air layer can improve the cooling effect of LWS. In addition, He et al. [235] found that compared with ordinary walls, LWS has better thermal insulation performance and the ability to cool local air.

Different plants have different characteristics including species, LAI, intensity, foliage thickness, etc., among which LAI and foliage thickness are considered to be the most important factors affecting the thermal performance of VGS. Dahanayake et al. [228] found that VGS could reduce the maximum external wall surface temperature by 12 °C when LAI increased from 1 to 5. By comparison of foliage thickness, Li et al. [236] found that plant leave with thickness of 19.8 cm have stronger convection heat transfer. Besides, the maximum surface temperature of the wall with VGS decreases by 6.3 °C compared with a bare wall.

Orientation, climate, and weather contribute significantly to the thermal performance of VGS. Pan et al. [237] found that the air temperature of the test room with VGS is 3.6 °C lower than that without VGS, and the VGS in the west-facing facade showed the best cooling performance, which gives the greatest wall temperature reduction (6.1 °C). Yang et al. [238] investigated the cooling effect of DSGF in Shanghai, the results showed that the cooling effect of the south-facing facade VGS is better, and the indoor air temperature drops by 1.2 °C on average. By analyzing DSGF and the original exposed masonry facades, it was discovered that the maximum air temperature drop in a daily circle is 5.5 °C. Furthermore, Xing et al. [239] found that in winter, DSGF can increase the indoor air temperature 1.0–3.0 °C at night and can achieve an 18.0% saving rate of heating energy consumption.

5.2. Urban Morphology

Urban planning determines urban morphology and affects urban climate, on the contrary, the urban climate can be adjusted and improved by means of urban planning to meet the needs of residents [240]. Urban planning and urban design have realistic environmental significance to mitigate the UHI effect of certain urban areas by manipulating or optimizing the urban morphology [241,242]. Urban size, urban geometric form, and vegetation coverage are the most basic urban morphology factors that affect the urban thermal environment [243].

Recent studies analyzed the impact of urban morphology parameters on the UHI effect in China. Hu et al. [242] found that the density of an urban area is the decisive factor influencing the UHII, the higher the density of the urban area, the higher the UHII. In addition, it was pointed out that contrary to the discrete morphology, the compact morphology with a larger average SVF value in the whole area may be more conducive to the reduction of the UHI effect. Wei et al. [244] investigated the impact of urban morphology parameters (such as SVF, floor area ratio, site coverage ratio, and building stories) on urban microclimate, and discovered that building site coverage of 25% is the best choice to mitigate the summer night UHI effect. Lin et al. [245] reported a higher floor area ratio, building density, and tree cover ratio may help to reduce daytime UHII in high-rise high-density urban environments. Tong et al. [246] found that the location close to tall buildings is more easily sheltered, and SVF is usually lower, which helps cool the environment during the day. In contrast, at night, air temperatures tend to accumulate in narrow street canyons with high-rise buildings and low SVF, which helps exacerbate the UHI effect. The research results of Zhou et al. [190] showed that building density has the greatest influence on UHII, followed by volume ratio and greenness rate. Similarly, Xu et al. [247] confirm that the green cover ratio can explain approximately 50% of the variability of UHII. Yue et al. [135] found that UHI was significantly correlated with urban configurations in two aspects. First, if the total building area remains constant, the smaller the building area is, the more dispersed it is, and the smaller the UHI is. Secondly, UHII can also be alleviated by a single patch of more complex shape.

The temperature varies greatly in the urban canopy and is very sensitive to the urban form. Tong et al. [246] found that increasing the number of buildings and narrowing

the pavement width could reduce daily maximum and daytime average temperature and increase daily average, daily minimum, and the nighttime average temperature in summer. In winter, daily average, daily minimum, and nighttime average temperatures are affected by urban morphology parameters. Specifically, they increase with the increase of buildings and the narrowing of street width. In addition, increasing the green plot ratio contributes to a daily minimum and nighttime average temperature reduction. Guo et al. [134] found that the urban form with medium height and low-density buildings is more able to cause LST changes compared with high-rise and high-density building arrays. Furthermore, building density has a greater impact on LST compared to building height. The combination of medium SVF values with relatively large vegetation area helps to produce a cooler environment, while the largest and smallest SVF values produce the highest LST. Huang et al. [248] found that the composition and configuration of the building are closely related to LST, the scattered distribution helps to mitigate LST, and the highest LST usually appears in commercial and industrial zones, which is consistent with the research results of Yue et al. [135]. In addition, Yin et al. [73] also confirmed that urban form factors have a significant impact on LST, and the analysis of the relationship between urban form and UHI effect based on regulatory program management unit is helpful to promote corresponding mitigation measures in practice.

5.3. Cool Material

It is well known that the UHI effect is highly related to urban geometry and urban materials. Once the urban form is established, it is difficult to change the permanence [249]. In contrast, the use of light-colored, low-thermal materials can be applied in urban areas to mitigate the overheating effect of UHI on urban microclimates [249].

5.3.1. Cool Roof and Cool Coatings on Building Surfaces

Cool roofs are defined as a roof with high solar reflectance and high thermal emissivity [250]. Gao et al. [251] found that roofs with white coating in Chongqing and Guangdong province can reduce their surface temperatures by about 20 °C and 17 °C respectively. Consequently, replacing grey roofs (reflectivity 0.2) with white ones (reflectivity 0.6) can save energy costs in hot summer cities, such as Chongqing, Shanghai, Wuhan, and Guangzhou. Compared to traditional materials, Han et al. [252] found that cool coatings applied to the roof can achieve an indoor temperature difference of more than 4.5 °C. Lu et al. [253] introduced a novel cool roof coupled with phase change materials and cool materials, and it has been proven that the novel cool roof has a good effect on thermal insulation and decreases the peaks of temperature, as confirmed through field testing. In addition, as an important measure to alleviate the UHI effect, cool roofs are recommended in China's relevant green building evaluation standards [250].

The solar irradiance incident on the traditional diffuse reflective surface is reflected in the urban canyon many times, which increases the absorption of the sun by the urban buildings and exacerbates the UHII effect [254,255]. The application of retro-reflective materials on architectural coatings or blocks has the potential to reduce heat intake from urban surfaces and mitigate the UHI effect. Qin et al. [254] found that the retro-reflective materials have better performance than diffuse ones in building blocks. Meng et al. [256] found that the peak temperature of the indoor air and inner wall surfaces were decreased up to 8 °C and 10 °C, respectively, due to the covering of retro-reflective materials, and the peak temperature of the outer wall surface is reduced up to 25 °C.

5.3.2. Cool Pavement

Pavement surface has changed the original thermal properties of the natural ground surface, and as the surface temperature of the road increases, the air temperature near the road increases, causing the UHI effect [257,258]. It is important to reduce the road temperature by using cold pavement instead of traditional pavement to reduce the UHI effect [14]. The existing cooling methods mainly include increasing the solar reflectance,

enhancing evaporation, reducing the sensible heat transfer of the urban atmosphere, or modifying the pavements [259,260]. Terms associated with cold pavements are reflective pavements, evaporative pavements, and heat-harnessing pavements [259]. Albedo is an important index to the radiation reflectivity of pavement surface, which is negatively correlated with the pavement surface temperature [14,261]. However, the use of reflective pavements to mitigate UHI on streets surrounded by tall buildings is ineffective compared to open streets [257]. Furthermore, Qin et al. [262] recommended that reflective pavements be used when the aspect ratio of the urban canyon is less than 1.0. Jiang et al. [258] designed a solar reflective coating for cooling asphalt pavements, and experimental results showed that the surface temperature reduction is about 8.5 °C to 9.5 °C. Chen et al. [263] found that the surface peak temperature of highly conductive concrete pavement can be 13 °C lower than that of conventional concrete pavement.

As another potential type of cool pavement, the permeable pavement has many environmental benefits beyond the traditional impermeable pavement. The evaporation rate is an important factor that affects the evaporative cooling effect of permeable pavement. Liu et al. [260] found that evaporation-enhanced permeable pavement has a great contribution to UHI mitigation, with a maximum cooling of 9.4 °C compared with traditional permeable pavement.

In addition, cool pavement can reduce the heat released by the road and improve the comfort of pedestrians and nearby residents by reducing the heat storage capacity. Du et al. [264] found that the strategy of cooling asphalt pavement by increasing solar absorption of asphalt pavement and accelerating heat release to the base layer can reduce the surface and internal temperatures by 3.5 °C and 6.4 °C, respectively. Jiang et al. [265] designed a road thermo-electric generator system, which can convert or transfer the pavement heat, lowering the surface temperature by 8–9 °C during the summer.

5.4. Water Bodies

Water bodies are one of the main components of the urban areas, with their high thermal capacity and low thermal conductivity, which can effectively mitigate the UHI effect [51,123,266]. The cooling effect of urban water bodies, which is considered an important ecosystem regulation service, has many potential advantages, such as reducing energy consumption, improving the thermal comfort of pedestrians in the outdoor environment, and creating UCI [51,267,268].

Urban water bodies mainly include rivers, lakes, and reservoirs, forming a large part of the UCI [269]. Yang et al. [266] pointed out that rivers and lakes in Bozhou, China, are the main source of urban cooling in the summer. Wang et al. [270] found that wetland has a good regulation effect on temperature and the closer to the urban wetland, the more significant the temperature regulation. Xue et al. [271] pointed out that the average normalized cooling capability index (NCCI) of wetlands in Changchun city is 42.3 times that of green land, and the average NCCI value of wetlands connected to other surface waters was 6 times higher than that of isolated wetlands. Among them, the cooling effect of the river is obviously higher than that of other wetland types. Du et al. [194] found that urban rivers change the flow of air around them, and the UHII nearby the river is lower. By studying the influence of artificial ponds on the urban thermal environment using experiment methods, Syafii et al. [268] found that the thermal environment with a pond is better than that without a pond, especially during the daytime, and ponds configured with larger surface areas showed greater cooling effects. Xu et al. [272] concluded that the cooling effect was more significant near the center of the water body, with the maximum value exceeding 0.8 °C. Furthermore, Du et al. [200] found that the UCI of faceted water bodies is stronger than linear ones.

In Shanghai, research was carried out to resolve the following problems: how strong the water-cooling island (WCI) effect is and how much temperature reduction is [123]. It is found that water bodies can reduce the ambient temperature by 3.32 °C. Moreover, geometry, the proportion of green area, and impervious surface are key factors for the

WCI effect. For a fixed area of the water body, the simple geometry, the large share of vegetation, and the small proportion of impervious surfaces help to achieve good WCI effects [123]. Sun et al. [273] conducted a quantitative study on UCII of 197 water bodies in Beijing and found that the mean UCII of the water body is 0.54 °C/100m. Furthermore, it is suggested that the area, shape, and location of water bodies are important indicators of UCII in urban areas which should be considered in quantifying microclimate regulation services and mitigating UHI effects [273,274]. Cai et al. [275] found that the cooling effect of water bodies can reach 1 km. Wu et al. [276] investigated the temperature fields around the reservoirs and the influencing factors in the Pearl River Delta area. The results indicated that the distance, type of underlying surface, and capacity have significant effects on the temperature field around the reservoirs. The temperature and distance between 0–100 m and 0–200 m from the boundary of the reservoirs show a linear relationship, and as the temperature increases, the influence of the reservoirs on the temperature gradually weakens when the distance exceeds 200 m.

5.5. Urban Ventilation

Urban ventilation takes the advantage of wind characteristics to bring fresh air from the suburbs into the city, which has been reported to be one of the main mitigation strategies to alleviate the UHI effect [277,278]. In addition to heat removal, urban ventilation is also important for improving the quality of the living environment, eliminating air pollution, and saving energy [278,279]. For example, in a new district of Shenzhen, the actual urban development did not use the original ventilation scheme, which leads to the blocking of wind channels and intensifies the UHI effect [280]. Given that the increase of near-surface aerosol pollution in Chinese cities and the frequent occurrence of haze during wintertime of China, and the UHI effect are related to the poor ventilation in cities, urban ventilation planning is very necessary [278,281].

Xu et al. [282] analyzed the spatial distribution of UHI and cool source based on the distribution map of the daily average temperature of typical meteorological conditions and put forward the proposal of planning urban ventilation channels to alleviate UHI. Furthermore, the location, quantity, and planning control requirements of urban ventilation corridors in the new urban districts are proposed by Su et al. [278]. Luo et al. [280] put forward suggestions on optimization urban ventilation from the aspects of road orientation, building layout, green space layout, and open recreation space by a case study in Lipu County of Guangxi. Based on the urban sprawl pattern of Dalian city with high density, which leads to the annually decreasing trend of wind speed, Guo et al. [283] evaluated the natural ventilation performance of different building forms by the CFD simulation tool. The results showed that urban enclosures, such as the row of strip apartments and high-rise buildings with large platforms, are not conducive to natural ventilation, while valid planning and measures like open space, ventilation channel, increasing the building height appropriately, reduction of low-rise large platform, adoption of streamlined building shape and reduction of building facade area have significant effects on promoting ventilation and alleviating UHI effect. In addition, non-uniform building height has worse ventilation performance than homogeneous building in the case of low density, while in the case of high density the ventilation performance is opposite [284].

Qiao et al. [285] suggested that urban design based on urban form and building height, considering wind direction and wind frequency, is effective for optimizing ventilation and regulating the urban environment. Du et al. [194] found that wind speed near rivers is higher than that in urban centers where buildings are dense and suggested that it should be fully considered that how to guide the development of wind direction from rivers to interior areas, and how to expand the influence area of rivers, so as to optimize the urban thermal environment. Combined with the national technical guide "Specifications for climatic feasibility demonstration-Urban Ventilation Corridor", Ren et al. [281] proposed the ventilation corridor planning in Chinese cities.

6. Discussion

The impact of UHI on building energy demands has been studied in many large cities in China. Generally speaking, the UHI effect will increase the annual energy consumption of buildings in the areas dominated by air-conditioning. On the contrary, the UHI effect reduces the annual energy consumption of buildings in the areas dominated by heating. In addition, the extent to which UHI affects building energy demands depends on the local microclimate and urban features of the area, where the building is located, while for buildings in the same area, the energy consumption is also affected by the type and characteristics of the building, refrigeration/heating equipment, etc. However, although the importance of the impact of UHI on building energy consumption is widely recognized, it may be inaccurate to estimate the energy consumption of buildings located in the city center without considering their close relationship to other surrounding buildings or using meteorological data from suburban or rural weather stations. Enhanced government supervision strategies, which have shown a huge advantage in promoting building energy efficiency and mitigating UHI effects in Ningbo, are applicable to other cities of China [182].

UGS can improve the microclimate and alleviates the UHI phenomenon by shading and evapotranspiration, while the loss of urban vegetation cover and the reduced density of green in the urban environment is an important factor causing the phenomenon of UHI. Many studies have shown that UGS creates a UCI that is larger than its own boundaries during the daytime of summer. Considering the warming effect of trees inside UGS at night, it is recommended that less than 50% of the paving area and at least 30% of UGS should be designed in open spaces for commercial areas, while more trees are suggested to be designed in open spaces at residential area [196]. In addition, increasing undergrowth vegetation coverage and strengthening grassland irrigation management can bring into play the cooling effect of UGS. The cooling effect of UGS also depends largely on plant type, canopy density, and its own shape and area, etc. However, the Chinese public and urban managers often underestimate the cooling effect of UGS due to a lack of this information. Despite all this, a series of policies have been formulated in China to maintain and indeed introduce more UGS into cities, such as "Regulations of China on Urban Greening" and "Regulations on the greening of provinces and municipalities in China", and policymakers have developed measures to identify and understand UGS dynamics [286].

Many studies have proven that GR has a significant cooling effect on non-insulated buildings and is an effective way to increase the greenery coverage and reduce the UHI effect, especially in built-up urban areas. However, GR has not been widely adopted in some high-density cities in China (Beijing, Hong Kong, etc.) as some urban residents are reluctant to invest in GR and the government lacks incentives. It is therefore important for decision-makers to play a leading role in promoting GR related codes, policies, and incentives, such as in Shanghai, where the government has stipulated that more than 30% of the available roof area of new public buildings should be covered by GR since 2015 [217]. In addition, the indoor temperature of GR is higher than that for traditional roofs at night, the combination of GR with night-time ventilation can effectively reduce the indoor temperature. Currently, most studies in China have focused on the LAI and the types and heat transfer characteristics of GR, but no consensus has been reached on specific characteristics of GR, such as the quantity and spatial structure of green cover and types of soil or plant, etc. [204,240].

VGS may have a greater impact on the built environment than GR, given that the surface area of building walls is always greater than the area of the roof, especially the high wall to roof ratio for high-rise buildings can offer larger areas for planting. However, studies have shown that greening of the facade surface area by 30–50% only reduces the air temperature by about 1.0 °C in the high-density urban environment [287]. It is also important to note that VGS may increase the building's heating needs during winter. In addition, VGS is controversial in terms of its cost and the complexity of its implementation, and a more systematic understanding of its practical application in future research is needed.

Urban morphology can change urban energy balance, thus affecting the urban microclimate. The denser and more complex the urban area, the greater the UHII is. Therefore, large cities could have a stronger UHI effect than smaller cities. Specifically, urban morphology indexes such as building density, SVF, and floor area ratio are closely related to the UHI effect. Building density has proven to be an important indicator that affects the UHI, and reasonable planning of building density can increase airflow and heat dissipation in cities. Considering the relatively high negative correlation between SVF and UHI, SVF values can be used to infer the potential UHI impact of the planning for areas. In addition, some reasonable ranges of urban morphological indicators value are given by Xu et al. [247], such as building footprint ratio $\leq$23.8%, green cover ratio $\geq$30%, and green space ratio $\geq$19.5%. However, there is still a lack of understanding of the relationship between urban morphology indicators and UHI in some respects, such as the existing models failing to consider the interaction and nonlinear relationship between these indicators, or the fact that non-urban climate impacts were not removed when studying the effects of urban morphology on UHI.

Cool roofs are capable of effectively reflecting solar radiation and emitting heat and can therefore reduce the cooling energy use of buildings during the summer. Considering that the performance of the cool roof is mainly affected by the climatic conditions and the construction characteristics, the adoption of cool roofs instead of standard ones in northern Chinese cities may increase the demand for heating energy in winter. Moreover, the application of cool materials on external surfaces and pavement can decrease the ambient temperature around the buildings and reduce the surface temperature of the ground to improve the urban thermal conditions. Given that the variety of climate types in China, cool materials are more suitable for hot climatic cities. Therefore, the potential and cost of using cool materials to mitigate UHI must be carefully weighed in practice.

As natural cold sources, water bodies and ventilation are also important to mitigate the effects of UHI. Water bodies not only have a low surface temperature but also reduce the surrounding environment temperature because of their characteristics of low reflectivity and efficient consumption of short-wave radiation by evaporation. The cooling effect of the water body could be better if it is combined with UGS. It is worth noting that the cooling effect of the water body is influenced by the area, shape, and location of water bodies, landscape shape index, and the proportion of surrounding buildings. Moreover, enhanced ventilation can significantly improve the urban thermal environment and lead to the effective diffusion of pollutants. The water body, UGS, and dispersed cold air, etc., can play a better cooling effect under the connection of air channels. Hsieh et al. [277] suggested that urban planning should be reviewed taking into account the limitations of the leading-edge areas of buildings along the urban cooling route and the wind connections between the park and the river in order to mitigate the UHI effect. In addition, given the lack of communication between meteorological departments and urban planning departments, and the lack of relevant meteorological knowledge and simulation technology among planners and architects, Chinese scholars rarely study the UHI effect from the perspective of urban planning, which is a question worthy of careful consideration by decision-makers and relevant departments.

7. Conclusions

In this paper, we employed a comprehensive and systematic review of the current research status of UHI in China, including research methods, the impacts of UHI on building energy consumption, and mitigation strategies of UHI. The main conclusions are given below:

(1) In these research methods for studying UHI, the meteorological data methods are usually used to study long-term UHI phenomena in cities, whereas the fixed measurements or mobile traverse methods can directly collect the micro-climatic parameters and thus can obtain high-quality historical time series of temperature. Remote sensing methods provide an advantage that can get a large spatial distribution of UHI

considering the characteristics of satellite data with wide coverage and open access. Compared to other methods, numerical simulation methods have the advantage of performing comparative studies for different scenarios. The average annual SUHI is higher than CUHI in China. SUHII in the summer and winter days is higher in southern Chinese cities than that in northern cities, while SUHII in the summer and winter nights has the opposite geographic distribution.

(2) The formation, development, and evolution of UHI are influenced by many factors, including materials of buildings and open spaces, anthropogenic heat, evaporating surfaces, canyon geometry, and architectural design and layout, etc. Rising temperatures in cities could increase cooling energy consumption and seriously affect human health and well-being. To be specific, the UHI effect exacerbates cooling energy consumption in southern China, where the buildings are dominated by air conditioning, whereas in north China, where the heating in the winter is a major concern, the UHI effect helps reducing buildings energy consumption. The influence of UHI on building energy consumption is related to the local microclimate, the urban characteristics of the area where the building is located, and the type of building.

(3) The mitigation strategies to UHI in China, such as urban greening (including UGS, green roofs, and vertical greenery), urban morphology indicators, cool materials (including cool pavement, cool roof, and cool coatings on building surfaces), water bodies, and urban ventilation were reviewed and discussed. We found that UGS can form a cold island larger than its own boundary during the daytime of summer, and its cooling effect depends on vegetation types, canopy density, and the size and shape of UGS. Green roofs and vertical greenery have a significant cooling effect on the high-density buildings, and roof greening combined with night ventilation can significantly reduce indoor temperature and heat gain during the cooling period. Compared with cities in northern China, cool materials are more suitable for hot cities. It should be noted that green roofs, vertical greenery, and cool roofs have the potential to increase buildings' heating needs during winter. GR performs better than a cool roof in non-insulated buildings, while vertical greenery of high-rise buildings has a better cooling effect than the green roof. The cooling effect of water bodies is related to the area, shape, and location of water bodies, landscape shape index, and the proportion of the surrounding buildings. The cooling effect is better when the water combined with UGS or water and UGS are connected under ventilation channels. Urban morphology indicators, such as building density, SVF, floor area ratio, etc., have a strong relationship with the UHI effect. Therefore, the rational planning of these indicators hence can increase airflow and heat dissipation in cities.

In order to obtain greater urban environmental benefits, the cost and complexity of using these strategies to mitigate UHI should be carefully weighed in practice, and these mitigation strategies for UHI effect should be considered in the project design stage of urban planning and implemented on a large scale. In addition, it is important that more codes, policies, and incentives should be formulated in China to introduce more mitigation strategies into cities, and policymakers and urban managers should play a leading role in implementing these regulations.

Author Contributions: Y.L. reviewed the impact of UHI on building energy consumption in China. J.L. provided guidance on the methods of UHI and its status in China. J.W. is helpful to the English writing of this manuscript. L.T. reviewed the methods of studying UHI and its mitigation strategies and was a major contributor to the manuscript. All authors have read and agreed to the published version of the manuscript.

Funding: This research was funded by National Natural Science Foundation of China (No.51708054), Chengdu Science and Technology Project (No.2019-YF05-01377-SN), and the Fundamental Research Funds for the Central Universities (No.2018CDXYCH0015).

Institutional Review Board Statement: Not applicable.

Informed Consent Statement: Not applicable.

Data Availability Statement: Not applicable.

Conflicts of Interest: The authors declare no conflict of interest.

Nomenclature

ANN	Artificial neural network
BEM	Building energy models
BLUHI	Boundary layer urban heat island
CFD	Computational fluid dynamics
CLUHI	Canopy layer urban heat island
DGF	Direct green facade
DSGF	Double-skin green facade
EGR	Extensive green roof
FMMTM	Fixed measurements or mobile traverses methods
GR	Green roofs
IGR	Intensive green roof
ISA	Impervious surface area
ISAR	Impervious surface area ratio
LAI	Leaf area index
LULC	Land use and land cover
LST	Land surface temperature
LWS	Living walls system
MDM	Meteorological data methods
NCCI	Normalized cooling capability index
NDBI	Normalized difference building index
NDVI	Normalized difference vegetation index
NSM	Numerical simulation methods
NWP	Numerical weather prediction
PCI	Park cool island
RSM	Remote sensing methods
SEB	Surface energy balance
SUHI	Surface urban heat island
SVF	Sky view factors
UGS	Urban green spaces
UCI	Urban cool island
UCII	Urban cooling island intensity
UCMs	Urban canopy models
UHI	Urban heat island
UHII	Urban heat island intensity
VG	Vertical greening
VGS	Vertical greening system
WCI	Water cooling island
NDBI	Normalized difference building index

References

1. Jamei, Y.; Rajagopalan, P.; Sun, Q. Spatial structure of surface urban heat island and its relationship with vegetation and built-up areas in Melbourne, Australia. *Sci. Total Environ.* **2019**, *659*, 1335–1351. [CrossRef] [PubMed]
2. Mathew, A.; Khandelwal, S.; Kaul, N. Spatial and Temporal Variations of Urban Heat Island Effect and the effect of Percentage Impervious Surface Area and Elevation on Land Surface Temperature: Study of Chandigarh City, India. *Sustain. Cities Soc.* **2016**, *26*, 264–277. [CrossRef]
3. United Nations. *World Urbanization Prospects: The 2013 Revision*; United Nations: New York, NY, USA, 2014.
4. Marando, F.; Salvatori, E.; Sebastiani, A.; Fusaro, L.; Manes, F. Regulating Ecosystem Services and Green Infrastructure: Assessment of Urban Heat Island effect mitigation in the municipality of Rome, Italy. *Ecol. Model.* **2019**, *392*, 92–102. [CrossRef]
5. Sun, Y.; Gao, C.; Li, J.; Wang, R.; Liu, J. Evaluating urban heat island intensity and its associated determinants of towns and cities continuum in the Yangtze River Delta Urban Agglomerations. *Sustain. Cities Soc.* **2019**, *50*, 101659. [CrossRef]

6. Zhao, X.; Jiang, H.; Wang, H.; Zhao, J.; Qiu, Q.; Tapper, N.; Hua, L. Remotely sensed thermal pollution and its relationship with energy consumption and industry in a rapidly urbanizing Chinese city. *Energy Policy* **2013**, *57*, 398–406. [CrossRef]
7. Papamanolis, N. The main characteristics of the urban climate and the air quality in Greek cities. *Urban Clim.* **2015**, *12*, 49–64. [CrossRef]
8. Salvati, A.; Coch Roura, H.; Cecere, C. Assessing the urban heat island and its energy impact on residential buildings in Mediterranean climate: Barcelona case study. *Energy Build.* **2017**, *146*, 38–54. [CrossRef]
9. Taleghani, M. Outdoor thermal comfort by different heat mitigation strategies-A review. *Renew. Sustain. Energy Rev.* **2018**, *81*, 2011–2018. [CrossRef]
10. Nematchoua, M.K.; Yvon, A.; Roy, S.E.J.; Ralijaona, G.; Mamiharijaona, R.; Razafinjaka, J.N.; Tefy, R. A review on energy consumption in the residential and commercial buildings located in tropical regions of Indian Ocean: A case of Madagascar island. *J. Energy Storage* **2019**, *24*, 100748. [CrossRef]
11. Orimoloye, I.R.; Mazinyo, S.P.; Kalumba, A.M.; Ekundayo, O.Y.; Nel, W. Implications of climate variability and change on urban and human health: A review. *Cities* **2019**, *91*, 213–223. [CrossRef]
12. Qi, J.D.; He, B.J.; Wang, M.; Zhu, J.; Fu, W.C. Do grey infrastructures always elevate urban temperature? No, utilizing grey infrastructures to mitigate urban heat island effects. *Sustain. Cities Soc.* **2019**, *46*, 101392. [CrossRef]
13. Yang, X.; Yao, L.; Peng, L.L.H.; Jiang, Z.; Jin, T.; Zhao, L. Evaluation of a diagnostic equation for the daily maximum urban heat island intensity and its application to building energy simulations. *Energy Build.* **2019**, *193*, 160–173. [CrossRef]
14. Santamouris, M. Using cool pavements as a mitigation strategy to fight urban heat island-A review of the actual developments. *Renew. Sustain. Energy Rev.* **2013**, *26*, 224–240. [CrossRef]
15. Zinzi, M.; Carnielo, E. Impact of urban temperatures on energy performance and thermal comfort in residential buildings. The case of Rome, Italy. *Energy Build.* **2017**, *157*, 20–29. [CrossRef]
16. Li, X.; Zhou, Y.; Yu, S.; Jia, H.; Li, H.; Li, W. Urban heat island impacts on building energy consumption: A review of approaches and findings. *Energy* **2019**, *174*, 407–419. [CrossRef]
17. Ghobadi, A.; Khosravi, M.; Tavousi, T. Surveying of Heat waves Impact on the Urban Heat Islands: Case study, the Karaj City in Iran. *Urban Clim.* **2018**, *24*, 600–615. [CrossRef]
18. Kotharkar, R.; Ramesh, A.; Bagade, A. Urban Heat Island studies in South Asia: A critical review. *Urban Clim.* **2018**, *24*, 1011–1026. [CrossRef]
19. Ward, K.; Lauf, S.; Kleinschmit, B.; Endlicher, W. Heat waves and urban heat islands in Europe: A review of relevant drivers. *Sci. Total Environ.* **2016**, *569–570*, 527–539. [CrossRef]
20. Mavrogianni, A.; Davies, M.; Batty, M.; Belcher, S.E.; Bohnenstengel, S.I.; Carruthers, D.; Chalabi, Z.; Croxford, B.; Demanuele, C.; Evans, S.; et al. The comfort, energy and health implications of London's urban heat island. *Build. Serv. Eng. Res. T* **2011**, *32*, 35–52. [CrossRef]
21. Bowler, D.E.; Buyung-Ali, L.; Knight, T.M.; Pullin, A.S. Urban greening to cool towns and cities: A systematic review of the empirical evidence. *Landsc. Urban Plan.* **2010**, *97*, 147–155. [CrossRef]
22. Gago, E.J.; Roldan, J.; Pacheco-Torres, R.; Ordóñez, J. The city and urban heat islands: A review of strategies to mitigate adverse effects. *Renew. Sustain. Energy Rev.* **2013**, *25*, 749–758. [CrossRef]
23. Lai, D.; Liu, W.; Gan, T.; Liu, K.; Chen, Q. A review of mitigating strategies to improve the thermal environment and thermal comfort in urban outdoor spaces. *Sci. Total Environ.* **2019**, *661*, 337–353. [CrossRef]
24. Sun, R.; Lü, Y.; Yang, X.; Chen, L. Understanding the variability of urban heat islands from local background climate and urbanization. *J. Clean. Prod.* **2019**, *208*, 743–752. [CrossRef]
25. Zhou, D.; Zhao, S.; Liu, S.; Zhang, L. Spatiotemporal trends of terrestrial vegetation activity along the urban development intensity gradient in China's 32 major cities. *Sci. Total Environ.* **2014**, *488–489*, 136–145. [CrossRef] [PubMed]
26. Zhou, D.; Zhang, L.; Hao, L.; Sun, G.; Liu, Y.; Zhu, C. Spatiotemporal trends of urban heat island effect along the urban development intensity gradient in China. *Sci. Total Environ.* **2016**, *544*, 617–626. [CrossRef] [PubMed]
27. Mirzaei, P.A. Recent challenges in modeling of urban heat island. *Sustain. Cities Soc.* **2015**, *19*, 200–206. [CrossRef]
28. Morris, K.I.; Salleh, S.A.; Chan, A.; Ooi MC, G.; Abakr, A.; Oozeer, M.Y.; Duda, M. Computational study of urban heat island of Putrajaya, Malaysia. *Sustain. Cities Soc.* **2015**, *19*, 359–372. [CrossRef]
29. Effat, H.A.; Hassan, O.A.K. Change detection of urban heat islands and some related parameters using multi-temporal Landsat images; a case study for Cairo city, Egypt. *Urban Clim.* **2014**, *10*, 171–188. [CrossRef]
30. Santamouris, M. Analyzing the heat island magnitude and characteristics in one hundred Asian and Australian cities and regions. *Sci. Total Environ.* **2015**, *512–513*, 582–598. [CrossRef]
31. Zhao, S.; Zhou, D.; Liu, S. Data concurrency is required for estimating urban heat island intensity. *Environ. Pollut.* **2016**, *208*, 118–124. [CrossRef]
32. Jahangir, M.S.; Moghim, S. Assessment of the urban heat island in the city of Tehran using reliability methods. *Atmos. Res.* **2019**, *225*, 144–156. [CrossRef]
33. Ramakreshnan, L.; Aghamohammadi, N.; Fong, C.S.; Ghaffarianhoseini, A.; Ghaffarianhoseini, A.; Wong, L.P.; Hassan, N.; Sulaiman, N.M. A critical review of Urban Heat Island phenomenon in the context of Greater Kuala Lumpur, Malaysia. *Sustain. Cities Soc.* **2018**, *39*, 99–113. [CrossRef]

34. Oke, T.R. The heat island of the urban boundary layer: Characteristics, causes and effects. In *Wind Climate in Cities*; Cermak, J.E., Davenport, A.G., Plate, E.J., Viegas, D.X., Eds.; Kluwer Academic: Dordrecht, The Netherlands, 1995; pp. 81–107.
35. Voogt, J.A.; Oke, T.R. Complete urban surface temperatures. *J. Appl. Meteorol.* **1997**, *36*, 1117–1132. [CrossRef]
36. Deilami, K.; Kamruzzaman, M.; Liu, Y. Urban heat island effect: A systematic review of spatio-temporal factors, data, methods, and mitigation measures. *Int. J. Appl. Earth Obs. Geoinf.* **2018**, *67*, 30–42. [CrossRef]
37. Kotharkar, R.; Bagade, A. Evaluating urban heat island in the critical local climate zones of an Indian city. *Landsc. Urban Plan.* **2018**, *169*, 92–104. [CrossRef]
38. Luo, Y.; Li, Q.; Yang, K.; Xie, W.; Zhou, X.; Shang, C.; Xu, Y.; Zhang, Y.; Zhang, C. Thermodynamic analysis of air-ground and water-ground energy exchange process in urban space at micro scale. *Sci. Total Environ.* **2019**, *694*, 133612.
39. Mirzaei, P.A.; Haghighat, F. Approaches to study Urban Heat Island-Abilities and limitations. *Build. Environ.* **2010**, *45*, 2192–2201. [CrossRef]
40. Li, Z.L.; Tang, B.H.; Wu, H.; Ren, H.; Yan, G.; Wan, Z.; Trigo, I.F.; Sobrino, J. Satellite-derived land surface temperature: Current status and perspectives. *Remote Sens. Environ.* **2013**, *131*, 14–37. [CrossRef]
41. Song, J.; Du, S.; Feng, X.; Guo, L. The relationships between landscape compositions and land surface temperature: Quantifying their resolution sensitivity with spatial regression models. *Landsc. Urban Plan.* **2014**, *123*, 145–157. [CrossRef]
42. Shaker, R.R.; Altman, Y.; Deng, C.; Vaz, E.; Forsythe, K.W. Investigating urban heat island through spatial analysis of New York City streetscapes. *J. Clean. Prod.* **2019**, *233*, 972–992. [CrossRef]
43. Theophilou, M.K.; Serghides, D. Estimating the characteristics of the Urban Heat Island Effect in Nicosia, Cyprus, using multiyear urban and rural climatic data and analysis. *Energy Build.* **2015**, *108*, 137–144. [CrossRef]
44. Lazzarini, M.; Marpu, P.R.; Ghedira, H. Temperature-land cover interactions: The inversion of urban heat island phenomenon in desert city areas. *Remote Sens. Environ.* **2013**, *130*, 136–152. [CrossRef]
45. Rotem-Mindali, O.; Michael, Y.; Helman, D.; Lensky, I.M. The role of local land-use on the urban heat island effect of Tel Aviv as assessed from satellite remote sensing. *Appl. Geogr.* **2015**, *56*, 145–153. [CrossRef]
46. Lai, J.; Zhan, W.; Huang, F.; Quan, J.; Hu, L.; Gao, L.; Ju, W. Does quality control matter? Surface urban heat island intensity variations estimated by satellite-derived land surface temperature products. *ISPRS J. Photogramm. Remote Sens.* **2018**, *139*, 212–227. [CrossRef]
47. Levermore, G.; Parkinson, J.; Lee, K.; Laycock, P.; Lindley, S. The increasing trend of the urban heat island intensity. *Urban Clim.* **2018**, *24*, 360–368. [CrossRef]
48. Mathew, A.; Khandelwal, S.; Kaul, N.; Chauhan, S. Analyzing the diurnal variations of land surface temperatures for surface urban heat island studies: Is time of observation of remote sensing data important? *Sustain. Cities Soc.* **2018**, *40*, 194–213. [CrossRef]
49. Jin, M.; Shepherd, J.M.; Zheng, W. Urban Surface Temperature Reduction via the Urban Aerosol Direct Effect: A Remote Sensing and WRF Model Sensitivity Study. *Adv. Meteorol.* **2010**, *2010*, 1–14. [CrossRef]
50. Zhao, L.; Lee, X.; Smith, R.B.; Oleson, K. Strong contributions of local background climate to urban heat islands. *Nature* **2014**, *511*, 216–219. [CrossRef]
51. Sun, R.; Chen, A.; Chen, L.; Lü, Y. Cooling effects of wetlands in an urban region: The case of Beijing. *Ecol. Indic.* **2012**, *20*, 57–64. [CrossRef]
52. Rasul, A.; Balzter, H.; Smith, C. Spatial variation of the daytime Surface Urban Cool Island during the dry season in Erbil, Iraqi Kurdistan, from Landsat 8. *Urban Clim.* **2015**, *14*, 176–186. [CrossRef]
53. Rasul, A.; Balzter, H.; Smith, C. Diurnal and seasonal variation of surface urban cool and heat islands in the semi-arid city of Erbil. Iraq. *Climate* **2016**, *4*, 42. [CrossRef]
54. Rizvi, S.H.; Alam, K.; Iqbal, J. Spatio-temporal variations in urban heat island and its interaction with heat wave. *J. Atmos. Solar-Terr. Phys.* **2019**, *185*, 50–57. [CrossRef]
55. Yang, X.; Li, Y.; Luo, Z.; Chan, P.W. The urban cool island phenomenon in a high-rise high-density city and its mechanisms. *Int. J. Climatol.* **2016**, *37*, 890–904. [CrossRef]
56. Nunez, M.; Oke, T.R. The energy balance of urban canyon. *J. Appl. Meteorol.* **1977**, *16*, 11–19. [CrossRef]
57. Chen, S.; Hu, D.; Wong, M.S.; Ren, H.; Cao, S.; Yu, C.; Ho, H.C. Characterizing spatiotemporal dynamics of anthropogenic heat fluxes: A 20-year case study in Beijing-Tianjin-Hebei region in China. *Environ. Pollut.* **2019**, *249*, 923–931. [CrossRef]
58. Giridharan, R.; Emmanuel, R. The impact of urban compactness, comfort strategies and energy consumption on tropical urban heat island intensity: A review. *Sustain. Cities Soc.* **2018**, *40*, 677–687. [CrossRef]
59. Memon, R.A.; Leung, D.Y.C.; Liu, C.H. An investigation of urban heat island intensity (UHII) as an indicator of urban heating. *Atmos. Res.* **2009**, *94*, 491–500. [CrossRef]
60. Zeng, F.; Gao, N. Use of an Energy Balance Model for Studying Urban Surface Temperature at Microscale. *Procedia Eng.* **2017**, *205*, 2956–2966. [CrossRef]
61. Christen, A.; Voogt, R. Energy and radiation balance of a central European city. *Int. J. Climatol.* **2004**, *24*, 1395–1421. [CrossRef]
62. Brandsma, T.; Wolters, D. Measurement and Statistical Modeling of the Urban Heat Island of the City of Utrecht (the Netherlands). *J. Appl. Meteorol. Climatol.* **2012**, *51*, 1046–1060. [CrossRef]
63. Mohan, M.; Kikegawa, Y.; Gurjar, B.R.; Bhati, S.; Kandya, A.; Ogawa, K. Urban Heat Island Assessment for a Tropical Urban Airshed in India. *Atmos. Clim. Sci.* **2012**, *2*, 127–138. [CrossRef]

64. Hu, Y.; Hou, M.; Jia, C.; Zhen, X.; Xu, Y. Comparison of surface and canopy urban heat islands within megacities of eastern China. *ISPRS J. Photogramm. Remote Sens.* **2019**, *156*, 160–168. [CrossRef]
65. Yang, P.; Ren, G.; Hou, W. Impact of daytime precipitation duration on urban heat island intensity over Beijing city. *Urban Clim.* **2019**, *28*, 1–13. [CrossRef]
66. Grigoraș, G.; Urițescu, B. Land Use/Land Cover changes dynamics and their effects on Surface Urban Heat Island in Bucharest, Romania. *Int. J. Appl. Earth Obs. Geoinf.* **2019**, *80*, 115–126. [CrossRef]
67. Hong, J.W.; Hong, J.; Kwon, E.; Yoon, D.K. Temporal dynamics of urban heat island correlated with the socioeconomic development over the past half-century in Seoul, Korea. *Environ. Pollut.* **2019**, *254*, 112934. [CrossRef]
68. Pandey, A.K.; Singh, S.; Berwal, S.; Kumar, D.; Pandey, P.; Prakash, A.; Lodhi, N.; Maithani, S.; Jain, V.K.; Kumar, K. Spatio-temporal variations of urban heat island over Delhi. *Urban Clim.* **2014**, *10*, 119–133. [CrossRef]
69. Zhang, J.; Gou, Z.; Lu, Y.; Lin, P. The impact of sky view factor on thermal environments in urban parks in a subtropical coastal city of Australia. *Urban For. Urban Green.* **2019**, *44*, 126422. [CrossRef]
70. Qiao, Z.; Tian, G.; Xiao, L. Diurnal and seasonal impacts of urbanization on the urban thermal environment: A case study of Beijing using MODIS data. *ISPRS J. Photogramm. Remote Sens.* **2013**, *85*, 93–101. [CrossRef]
71. Toparlar, Y.; Blocken, B.; Vos, P.; Heijst, G.J.F.V.; Janssen, W.D.; Hooff, T.V.; Montazeri, H.; Timmermans, H.J.P. CFD simulation and validation of urban microclimate: A case study for Bergpolder Zuid, Rotterdam. *Build. Environ.* **2015**, *83*, 79–90. [CrossRef]
72. Soltani, A.; Sharifi, E. Daily variation of urban heat island effect and its correlations to urban greenery: A case study of Adelaide. *Front. Archit. Res.* **2017**, *6*, 529–538. [CrossRef]
73. Yin, C.; Yuan, M.; Lu, Y.; Huang, Y.; Liu, Y. Effects of urban form on the urban heat island effect based on spatial regression model. *Sci. Total Environ.* **2018**, *634*, 696–704. [CrossRef] [PubMed]
74. Busato, F.; Lazzarin, R.M.; Noro, M. Three years of study of the Urban Heat Island in Padua: Experimental results. *Sustain. Cities Soc.* **2014**, *10*, 251–258. [CrossRef]
75. Cao, Z.; Wu, Z.; Liu, L.; Chen, Y.; Zou, Y. Assessing the relationship between anthropogenic heat release warming and building characteristics in Guangzhou: A sustainable development perspective. *Sci. Total Environ.* **2019**, *695*, 133759. [CrossRef] [PubMed]
76. Xu, Y.; Zhou, D.; Li, Z. Research on Characteristic Analysis of Urban Heat Island in Multi-scales and Urban Planning Strategies. *Procedia Eng.* **2016**, *169*, 175–182. [CrossRef]
77. Li, H.; Zhou, Y.; Wang, X.; Zhou, X.; Zhang, H.; Sodoudi, S. Quantifying urban heat island intensity and its physical mechanism using WRF/UCM. *Sci. Total Environ.* **2019**, *650*, 3110–3119. [CrossRef]
78. Min, M.; Lin, C.; Duan, X.; Jin, Z.; Zhang, L. Spatial distribution and driving force analysis of urban heat island effect based on raster data: A case study of the Nanjing metropolitan area, China. *Sustain. Cities Soc.* **2019**, *50*, 101637. [CrossRef]
79. Zeleňáková, M.; Purcz, P.; Hlavatá, H.; Blišťan, P. Climate Change in Urban Versus Rural Areas. *Procedia Eng.* **2015**, *119*, 1171–1180. [CrossRef]
80. Founda, D.; Pierros, F.; Petakis, M.; Zerefos, C. Interdecadal variations and trends of the Urban Heat Island in Athens (Greece) and its response to heat waves. *Atmos. Res.* **2015**, *161–162*, 1–13. [CrossRef]
81. Hou, Y.; Chen, B.; Yang, X.; Liang, P. Observed Climate Change in East China during 1961–2007. *Adv. Clim. Chang. Res.* **2013**, *4*, 84–91.
82. Sun, Y.; Zhang, X.; Ren, G.; WZwiers, F.; Hu, T. Contribution of urbanization to warming in China. *Nat. Clim. Chang.* **2016**, *6*, 706–709. [CrossRef]
83. Jiang, S.; Wang, K.; Mao, Y. Rapid Local Urbanization around Most Meteorological Stations Explain the Observed Daily Asymmetric Warming Rates across China from 1985 to 2017. *J. Clim.* **2020**, *33*, 9045–9061. [CrossRef]
84. Yao, R.; Luo, Q.; Luo, Z.; Jiang, L.; Yang, Y. An integrated study of urban microclimates in Chongqing, China: Historical weather data, transverse measurement and numerical simulation. *Sustain. Cities Soc.* **2015**, *14*, 187–199. [CrossRef]
85. Li, G.; Zhang, X.; Mirzaei, P.A.; Zhang, J.; Zhao, Z. Urban heat island effect of a typical valley city in China: Responds to the global warming and rapid urbanization. *Sustain. Cities Soc.* **2018**, *38*, 736–745. [CrossRef]
86. Peng, S.; Feng, Z.; Liao, H.; Huang, B.; Peng, S.; Zhou, T. Spatial-temporal pattern of, and driving forces for, urban heat island in China. *Ecol. Indic.* **2019**, *96*, 127–132. [CrossRef]
87. Ramamurthy, P.; Sangobanwo, M. Inter-annual variability in urban heat island intensity over 10 major cities in the United States. *Sustain. Cities Soc.* **2016**, *26*, 65–75. [CrossRef]
88. Yang, W.; Wong, N.H.; Jusuf, S.K. Thermal comfort in outdoor urban spaces in Singapore. *Build. Environ.* **2013**, *59*, 426–435. [CrossRef]
89. Giannopoulou, K.; Livada, I.; Santamouris, M.; Saliari, M.; Assimakopoulos, M.; Caouris, Y.G. On the characteristics of the summer urban heat island in Athens, Greece. *Sustain. Cities Soc.* **2011**, *1*, 16–28. [CrossRef]
90. Kantzioura, A.; Kosmopoulos, P.; Zoras, S. Urban surface temperature and microclimate measurements in Thessaloniki. *Energy Build.* **2012**, *44*, 63–72. [CrossRef]
91. Liu, J.; Niu, J.; Xia, Q. Combining measured thermal parameters and simulated wind velocity to predict outdoor thermal comfort. *Build. Environ.* **2016**, *105*, 185–197. [CrossRef]
92. Dorigon, L.P.; Amorim, M.C. Spatial modeling of an urban Brazilian heat island in a tropical continental climate. *Urban Clim.* **2019**, *28*, 100461. [CrossRef]

93. Aflaki, A.; Mirnezhad, M.; Ghaffarianhoseini, A.; Ghaffarianhoseini, A.; Omrany, H.; Wang, Z.; Akbari, H. Urban heat island mitigation strategies: A state-of-the-art review on Kuala Lumpur, Singapore and Hong Kong. *Cities* **2017**, *62*, 131–145. [CrossRef]
94. Liu, L.; Lin, Y.; Liu, J.; Wang, L.; Wang, D.; Shui, T.; Chen, X.; Wu, Q. Analysis of local-scale urban heat island characteristics using an integrated method of mobile measurement and GIS-based spatial interpolation. *Build. Environ.* **2017**, *117*, 191–207. [CrossRef]
95. Wang, Y.; Ni, Z.; Chen, S.; Xia, B. Microclimate regulation and energy saving potential from different urban green infrastructures in a subtropical city. *J. Clean. Prod.* **2019**, *226*, 913–927. [CrossRef]
96. Yang, F.; Lau, S.S.Y.; Qian, F. Summertime heat island intensities in three high-rise housing quarters in inner-city Shanghai China: Building layout, density and greenery. *Build. Environ.* **2010**, *45*, 115–134. [CrossRef]
97. Jin, C.; Bai, X.; Luo, T.; Zou, M. Effects of green roofs' variations on the regional thermal environment using measurements and simulations in Chongqing, China. *Urban For. Urban Green.* **2018**, *29*, 223–237. [CrossRef]
98. Chen, Y.C.; Yao, C.K.; Honjo, T.; Lin, T.P. The application of a high-density street-level air temperature observation network (HiSAN): Dynamic variation characteristics of urban heat island in Tainan, Taiwan. *Sci. Total Environ.* **2018**, *626*, 555–566. [CrossRef] [PubMed]
99. El-Hattab, M.; Amany, S.M.; Lamia, G.E. GEL Monitoring and assessment of urban heat islands over the Southern region of Cairo Governorate, Egypt. *Egypt. J. Remote Sens. Space Sci.* **2018**, *21*, 311–323.
100. de Faria Peres, L.; de Lucena, A.J.; Rotunno Filho, O.C.; de Almeida França, J.R. The urban heat island in Rio de Janeiro, Brazil, in the last 30 years using remote sensing data. *Int. J. Appl. Earth Obs. Geoinf.* **2018**, *64*, 104–116. [CrossRef]
101. Shirani-Bidabadi, N.; Nasrabadi, T.; Faryadi, S.; Larijani, A.; Roodposhti, M.S. Evaluating the spatial distribution and the intensity of urban heat island using remote sensing, case study of Isfahan city in Iran. *Sustain. Cities Soc.* **2019**, *45*, 686–692. [CrossRef]
102. Rani, M.; Kumar, P.; Pandey, P.C.; Srivastava, P.K.; Chaudhary, B.S.; Tomar, V.; Mandal, V.P. Multi-Temporal NDVI and Surface Temperature Analysis for Urban Heat Island inbuilt surrounding of Sub-humid Region: A Case Study of two Geographical Regions. *Remote Sens. Appl. Soc. Environ.* **2018**, *10*, 163–172. [CrossRef]
103. Silva, J.S.; Silva, R.M.; Santos CA, G. Spatiotemporal impact of land use/land cover changes on urban heat islands: A case study of Paço do Lumiar, Brazil. *Build. Environ.* **2018**, *136*, 279–292. [CrossRef]
104. Yao, R.; Wang, L.; Huang, X.; Niu, Y.; Chen, Y.; Niu, Z. The influence of different data and method on estimating the surface urban heat island intensity. *Ecol. Indic.* **2018**, *89*, 45–55. [CrossRef]
105. Zhang, Y.; Sun, L. Spatial-temporal impacts of urban land use land cover on land surface temperature: Case studies of two Canadian urban areas. *Int. J. Appl. Earth Obs. Geoinf.* **2019**, *75*, 171–181. [CrossRef]
106. Dwivedi, A.; Khire, M.V. Application of Split-Window Algorithm to study Urban Heat Island Effect in Mumbai through Land Surface Temperature approach. *Sustain. Cities Soc.* **2018**, *41*, 865–877. [CrossRef]
107. Shi, Y.; Katzschner, L.; Ng, E. Modelling the fine-scale spatiotemporal pattern of urban heat island effect using land use regression approach in a megacity. *Sci. Total Environ.* **2017**, *618*, 891–904. [CrossRef]
108. Li, H.; Zhou, Y.; Li, X.; Meng, L.; Wang, X.; Wu, S.; Sodoudi, S. A new method to quantify surface urban heat island intensity. *Sci. Total Environ.* **2017**, *624*, 262–272. [CrossRef]
109. Wang, J.; Huang, B.; Fu, D.; Atkinson, P.M.; Zhang, X. Response of urban heat island to future urban expansion over the Beijing-Tianjin-Hebei metropolitan area. *Appl. Geogr.* **2016**, *70*, 26–36. [CrossRef]
110. Ye, C.; Liu, Y.; Quan, W.; Liu, W.; Liu, C. Application of Urban Thermal Environment Monitoring Based on Remote Sensing in Beijing. *Procedia Environ. Sci.* **2011**, *11*, 1424–1433.
111. Huang, F.; Zhan, W.; Voogt, J.; Hu, L.; Wang, Z.; Quan, J.; Ju, W.; Guo, Z. Temporal upscaling of surface urban heat island by incorporating an annual temperature cycle model: A tale of two cities. *Remote Sens. Environ.* **2016**, *186*, 1–12. [CrossRef]
112. Sheng, L.; Hu, H.; You, H.; Gu, Q.; Hu, H. Comparison of the urban heat island intensity quantified by using air temperature and Landsat land surface temperature in Hangzhou, China. *Ecol. Indic.* **2017**, *72*, 738–746. [CrossRef]
113. Yao, R.; Wang, L.; Huang, X.; Niu, Z.; Liu, F.; Wang, Q. Temporal trends of surface urban heat islands and associated determinants in major Chinese cities. *Sci. Total Environ.* **2017**, *609*, 742–754. [CrossRef] [PubMed]
114. Yao, R.; Wang, L.; Huang, X.; Zhang, W.; Li, J.; Niu, Z. Interannual variations in surface urban heat island intensity and associated drivers in China. *J. Environ. Manag.* **2018**, *222*, 86–94. [CrossRef] [PubMed]
115. Yue, W.; Qiu, S.; Xu, H.; Xu, X.; Zhang, L. Polycentric urban development and urban thermal environment: A case of Hangzhou, China. *Landsc. Urban Plan.* **2019**, *189*, 58–70. [CrossRef]
116. Zhou, D.; Zhao, S.; Liu, S.; Zhang, L.; Zhu, C. Surface urban heat island in China's 32 major cities: Spatial patterns and drivers. *Remote Sens. Environ.* **2014**, *152*, 51–61. [CrossRef]
117. Liu, S.; Zang, Z.; Wang, W.; Wu, Y. Spatial-temporal evolution of urban heat Island in Xi'an from 2006 to 2016. *Phys. Chem. Earth* **2019**, *110*, 185–194. [CrossRef]
118. Zhang, H.; Qi, Z.; Ye, X.; Cai, Y.; Ma, W. Analysis of land use/land cover change, population shift, and their effects on spatiotemporal patterns of urban heat islands in metropolitan Shanghai, China. *Appl. Geogr.* **2013**, *44*, 121–133. [CrossRef]
119. Meng, Q.; Zhang, L.; Sun, Z.; Meng, F.; Wang, L.; Sun, Y. Characterizing spatial and temporal trends of surface urban heat island effect in an urban main built-up area: A 12-year case study in Beijing, China. *Remote Sens. Environ.* **2017**, *204*, 826–837. [CrossRef]
120. Lin, Y.; Jim, C.Y.; Deng, J.; Wang, Z. Urbanization effect on spatiotemporal thermal patterns and changes in Hangzhou (China). *Build. Environ.* **2018**, *145*, 166–176. [CrossRef]

121. Yu, Z.; Yao, Y.; Yang, G.; Wang, X.; Vejre, H. Spatiotemporal patterns and characteristics of remotely sensed region heat islands during the rapid urbanization (1995–2015) of Southern China. *Sci. Total Environ.* **2019**, *674*, 242–254. [CrossRef]
122. Kong, F.; Yin, H.; James, P.; Hutyra, L.R.; He, H.S. Effects of spatial pattern of greenspace on urban cooling in a large metropolitan area of eastern China. *Landsc. Urban Plan.* **2014**, *128*, 35–47. [CrossRef]
123. Du, H.; Song, X.; Jiang, H.; Kan, Z.; Wang, Z.; Cai, Y. Research on the cooling island effects of water body: A case study of Shanghai, China. *Ecol. Indic.* **2016**, *67*, 31–38. [CrossRef]
124. Sun, R.; Chen, L. Effects of green space dynamics on urban heat islands: Mitigation and diversification. *Ecosyst. Serv.* **2017**, *23*, 38–46. [CrossRef]
125. Cai, Y.; Chen, Y.; Tong, C. Spatiotemporal evolution of urban green space and its impact on the urban thermal environment based on remote sensing data: A case study of Fuzhou City, China. *Urban For. Urban Green.* **2019**, *41*, 333–343. [CrossRef]
126. Wang, W.; Liu, K.; Tang, R.; Wang, S. Remote sensing image-based analysis of the urban heat island effect in Shenzhen, China. *Phys. Chem. Earth* **2019**, *110*, 168–175. [CrossRef]
127. Li, J.; Song, C.; Cao, L.; Zhu, F.; Meng, X.; Wu, J. Impacts of landscape structure on surface urban heat islands: A case study of Shanghai, China. *Remote Sens. Environ.* **2011**, *115*, 3249–3263. [CrossRef]
128. Wu, H.; Ye, L.; Shi, W.; Clarke, K.C. Assessing the effects of land use spatial structure on urban heat islands using HJ-1B remote sensing imagery in Wuhan, China. *Int. J. Appl. Earth Obs. Geoinf.* **2014**, *32*, 67–78. [CrossRef]
129. Du, H.; Wang, D.; Wang, Y.; Zhao, X.; Qin, F.; Cai, Y. Influences of land cover types, meteorological conditions, anthropogenic heat and urban area on surface urban heat island in the Yangtze River Delta Urban Agglomeration. *Sci. Total Environ.* **2016**, *571*, 461–470. [CrossRef]
130. Xu, D.; Chen, R. Comparison of urban heat island and urban reflection in Nanjing City of China. *Sustain. Cities Soc.* **2017**, *31*, 26–36. [CrossRef]
131. Dai, Z.; Guldmann, J.M.; Hu, Y. Spatial regression models of park and land-use impacts on the urban heat island in central Beijing. *Sci. Total Environ.* **2018**, *626*, 1136–1147. [CrossRef]
132. Yu, Z.; Yao, Y.; Yang, G.; Wang, X.; Vejre, H. Strong contribution of rapid urbanization and urban agglomeration development to regional thermal environment dynamics and evolution. *For. Ecol. Manag.* **2019**, *446*, 214–225. [CrossRef]
133. Chen, W.; Zhang, Y.; Gao, W.; Zhou, D. The Investigation of Urbanization and Urban Heat Island in Beijing Based on Remote Sensing. *Procedia Soc. Behav. Sci.* **2016**, *216*, 141–150. [CrossRef]
134. Guo, G.; Zhou, X.; Wu, Z.; Xiao, R.; Chen, Y. Characterizing the impact of urban morphology heterogeneity on land surface temperature in Guangzhou, China. *Environ. Model. Softw.* **2016**, *84*, 427–439. [CrossRef]
135. Yue, W.; Liu, X.; Zhou, Y.; Liu, Y. Impacts of urban configuration on urban heat island: An empirical study in China mega-cities. *Sci. Total Environ.* **2019**, *671*, 1036–1046. [CrossRef]
136. Zhou, D.; Bonafoni, S.; Zhang, L.; Wang, R. Remote sensing of the urban heat island effect in a highly populated urban agglomeration area in East China. *Sci. Total Environ.* **2018**, *628*, 415–429. [CrossRef]
137. Li, Z.; Liu, L.; Dong, X.; Liu, J. The study of regional thermal environments in urban agglomerations using a new method based on metropolitan areas. *Sci. Total Environ.* **2019**, *672*, 370–380. [CrossRef]
138. Chang, H.; Xiang, C.; Duan, C.; Wan, Z.; Liu, Y.; Zheng, Y.; Shang, Y.; Liu, M.; Shu, S. Study on the thermal performance and wind environment in a residential community. *Int. J. Hydrogen Energy* **2016**, *41*, 15868–15878. [CrossRef]
139. Li, X.X.; Norford, L.K. Evaluation of cool roof and vegetations in mitigating urban heat island in a tropical city, Singapore. *Urban Clim.* **2016**, *16*, 59–74. [CrossRef]
140. Toparlar, Y.; Blocken, B.; Maiheu, B.; van Heijst, G.J.F. A review on the CFD analysis of urban microclimate. *Renew. Sustain. Energy Rev.* **2017**, *80*, 1613–1640. [CrossRef]
141. Morini, E.; Touchaei, A.G.; Rossi, F.; Cotana, F.; Akbari, H. Evaluation of albedo enhancement to mitigate impacts of urban heat island in Rome (Italy) using WRF meteorological model. *Urban Clim.* **2018**, *24*, 551–566. [CrossRef]
142. Liu, X.; Tian, G.; Feng, J.; Wang, J.; Kong, L. Assessing summertime urban warming and the cooling efficacy of adaptation strategy in the Chengdu-Chongqing metropolitan region of China. *Sci. Total Environ.* **2018**, *610*, 1092–1102. [CrossRef]
143. Giannaros, T.M.; Melas, D.; Daglis, I.A.; Keramitsoglou, I.; Kourtidis, K. Numerical study of the urban heat island over Athens (Greece) with the WRF model. *Atmos. Environ.* **2013**, *73*, 103–111. [CrossRef]
144. Tsoka, S.; Tsikaloudaki, A.; Theodosiou, T. Analyzing the ENVI-met microclimate model's performance and assessing cool materials and urban vegetation applications-a review. *Sustain. Cities Soc.* **2018**, *43*, 55–76. [CrossRef]
145. Garuma, G.F. Review of urban surface parameterizations for numerical climate models. *Urban Clim.* **2017**, *24*, 830–851. [CrossRef]
146. Battista, G.; de Lieto Vollaro, R.; Zinzi, M. Assessment of urban overheating mitigation strategies in a square in Rome, Italy. *Solar Energy* **2019**, *180*, 608–621. [CrossRef]
147. Wang, Y.; Berardi, U.; Akbari, H. Comparing the effects of Urban Heat Island Mitigation Strategies for Toronto, Canada. *Energy and Build.* **2015**, *114*, 2–19. [CrossRef]
148. Allegrini, J.; Dorer, V.; Carmeliet, J. Influence of morphologies on the microclimate in urban neighbourhoods. *J. Wind Eng. Ind. Aerodyn.* **2015**, *144*, 108–117. [CrossRef]
149. Allegrini, J.; Carmeliet, J. Simulations of local heat islands in Zürich with coupled CFD and building energy models. *Urban Clim.* **2017**, *24*, 340–359. [CrossRef]

150. Allegrini, J.; Orehounig, K.; Mavromatidis, G.; Ruesch, F.; Dorer, V.; Evins, R. A review of modelling approaches and tools for the simulation of district-scale energy systems. *Renew. Sustain. Energy Rev.* **2015**, *52*, 1391–1404. [CrossRef]
151. Wong, M.S.; Nichol, J.E.; To, P.H.; Wang, J. A simple method for designation of urban ventilation corridors and its application to urban heat island analysis. *Build. Environ.* **2010**, *45*, 1880–1889. [CrossRef]
152. Touchaei, A.G.; Wang, Y. Characterizing urban heat island in Montreal (Canada)-Effect of urban morphology. *Sustain. Cities Soc.* **2015**, *19*, 395–402. [CrossRef]
153. de Souza, D.O.; dos Santos Alvalá, R.C.; do Nascimento, M.G. Urbanization effects on the microclimate of Manaus: A modeling study. *Atmos. Res.* **2016**, *167*, 237–248. [CrossRef]
154. Takebayashi, H.; Senoo, M. Analysis of the relationship between urban size and heat island intensity using WRF model. *Urban Clim.* **2018**, *24*, 287–298. [CrossRef]
155. Taleb, D.; Abu-Hijleh, B. Urban heat islands: Potential effect of organic and structured urban configurations on temperature variations in Dubai, UAE. *Renew. Energy* **2013**, *50*, 747–762. [CrossRef]
156. Taleghani, M.; Sailor, D.J.; Tenpierik, M. Thermal assessment of heat mitigation strategies: The case of Portland State University, Oregon, USA. *Build. Environ.* **2014**, *73*, 138–150. [CrossRef]
157. Noro, M.; Lazzarin, R. Urban heat island in Padua, Italy: Simulation analysis and mitigation strategies. *Urban Clim.* **2015**, *14*, 187–196. [CrossRef]
158. O'Malley Christopher Piroozfar, P.; Farr, E.R.P.; Pomponi, F. Urban Heat Island (UHI) mitigating strategies: A case-based comparative analysis. *Sustain. Cities Soc.* **2015**, *19*, 222–235. [CrossRef]
159. Peron, F.; De Maria, M.M.; Spinazzè, F.; Mazzali, U. An analysis of the urban heat island of Venice mainland. *Sustain. Cities Soc.* **2015**, *19*, 300–309. [CrossRef]
160. Lin, B.S.; Lin, C.T. Preliminary study of the influence of the spatial arrangement of urban parks on local temperature reductionr. *Urban For. Urban Green.* **2016**, *20*, 348–357. [CrossRef]
161. Wang, Y.; Akbari, H. The effects of street tree planting on Urban Heat Island mitigation in Montreal. *Sustain. Cities Soc.* **2016**, *27*, 122–128. [CrossRef]
162. Lu, J.; Li, Q.; Zeng, L.; Chen, J.; Liu, G.; Li, Y.; Li, W.; Huang, K. A micro-climatic study on cooling effect of an urban park in a hot and humid climate. *Sustain. Cities Soc.* **2017**, *32*, 513–522. [CrossRef]
163. Herath, H.M.P.I.K.; Halwatura, R.U.; Jayasinghe, G.Y. Evaluation of green infrastructure effects on tropical Sri Lankan urban context as an urban heat island adaptation strategy. *Urban For. Urban Green.* **2018**, *29*, 212–222. [CrossRef]
164. Berardi, U. The outdoor microclimate benefits and energy saving resulting from green roofs retrofits. *Energy Build.* **2016**, *121*, 217–229. [CrossRef]
165. Heidarinejad, M.; Gracik, S.; Roudsari, M.S.; Nikkho, S.K.; Liu, J.; Liu, K.; Pitchorov, G.; Srebric, J. Influence of Building Surface Solar Irradiance on Environmental Temperatures in Urban Neighborhoods. *Sustain. Cities Soc.* **2016**, *26*, 186–202. [CrossRef]
166. Yang, Y.K.; Kang, I.S.; Chung, M.H.; Kim, S.; Park, J.C. Effect of PCM cool roof system on the reduction in urban heat island phenomenon. *Build. Environ.* **2017**, *122*, 411–421. [CrossRef]
167. Kolokotsa, D.; Santamouris, M.; Zerefos, S.C. Green and cool roofs' urban heat island mitigation potential in European climates for office buildings under free floating conditions. *Solar Energy* **2013**, *95*, 118–130. [CrossRef]
168. Rajagopalan, P.; Lim, K.C.; Jamei, E. Urban heat island and wind flow characteristics of a tropical city. *Solar Energy* **2014**, *107*, 159–170. [CrossRef]
169. Martin, M.; Afshari, A.; Armstrong, P.R.; Norford, L.K. Estimation of urban temperature and humidity using a lumped parameter model coupled with an EnergyPlus model. *Energy Build.* **2015**, *96*, 221–235. [CrossRef]
170. Gobakis, K.; Kolokotsa, D.; Synnefa, A.; Saliari, M.; Giannopoulou, K.; Santamouris, M. Development of a model for urban heat island prediction using neural network techniques. *Sustain. Cities Soc.* **2011**, *1*, 104–115. [CrossRef]
171. Lee, Y.Y.; Kim, J.T.; Yun, G.Y. The neural network predictive model for heat island intensity in Seoul. *Energy Build.* **2016**, *110*, 353–361. [CrossRef]
172. Parsaee, M.; Joybari, M.M.; Mirzaei, P.A.; Haghighat, F. Urban heat island, urban climate maps and urban development policies and action plans. *Environ. Technol. Innov.* **2019**, *14*, 100341. [CrossRef]
173. Hu, Z.; Yu, B.; Chen, Z.; Li, T.; Liu, M. Numerical investigation on the urban heat island in an entire city with an urban porous media model. *Atmos. Environ.* **2012**, *47*, 509–518. [CrossRef]
174. Schlünzen, K.H.; Grawe, D.; Bohnenstengel, S.I.; Schlüter, I.; Koppmann, R. Joint modelling of obstacle induced mesoscale changes-current limits challenges. *J. Wind Eng. Ind. Aerodyn* **2011**, *99*, 217–225. [CrossRef]
175. Ashtiani, A.; Mirzaei, P.A.; Haghighat, F. Indoor thermal condition in urban heat island: Comparison of the artificial neural network and regression methods prediction. *Energy Build.* **2014**, *76*, 597–604. [CrossRef]
176. Wang, Y.; Gu, A.; Zhang, A. Recent development of energy supply and demand in China, and energy sector prospects through 2030. *Energy Policy* **2011**, *39*, 6745–6759. [CrossRef]
177. Yan, Z.; Wang, J.; Xia, J.; Feng, J. Review of recent studies of the climatic effects of urbanization in China. *Adv. Clim. Chang. Res.* **2016**, *7*, 154–168. [CrossRef]
178. Li, L.; Chen, C.; Xie, S.; Huang, C.; Cheng, Z.; Wang, H.; Wang, Y.; Huang, H.; Lu, J.; Dhakal, S. Energy demand and carbon emissions under different development scenarios for Shanghai, China. *Energy Policy* **2010**, *38*, 4797–4807. [CrossRef]
179. Tan, Y.; Xu, H.; Zhang, X. Sustainable urbanization in China: A comprehensive literature review. *Cities* **2016**, *55*, 82–93. [CrossRef]

180. Yao, J.; Zhu, N. Enhanced supervision strategies for effective reduction of building energy consumption-A case study of Ningbo. *Energy Build.* **2011**, *43*, 2197–2202. [CrossRef]
181. Cui, Y.; Yan, D.; Hong, T.; Ma, J. Temporal and spatial characteristics of the urban heat island in Beijing and the impact on building design and energy performance. *Energy* **2017**, *130*, 286–297. [CrossRef]
182. Liu, L.; Liu, J.; Lin, Y. Spatial-temporal Analysis of the Urban Heat Island of a Subtropical City by Using Mobile Measurement. *Procedia Eng.* **2016**, *169*, 55–63. [CrossRef]
183. Cui, L.; Shi, J. Urbanization and its environmental effects in Shanghai, China. *Urban Clim.* **2012**, *2*, 1–15. [CrossRef]
184. Chen, F.; Yang, X.; Zhu, W. WRF simulations of urban heat island under hot-weather synoptic conditions: The case study of Hangzhou City, China. *Atmos. Res.* **2014**, *138*, 364–377. [CrossRef]
185. Saadatian, O.; Sopian, K.; Salleh, E.; Lim, C.H.; Riffat, S.; Saadatian, E.; Toudeshki, A.; Sulaiman, M.Y. A review of energy aspects of green roofs. *Renew. Sustain. Energy Rev.* **2013**, *23*, 155–168. [CrossRef]
186. Wong, S.L.; Wan, K.K.W.; Yang, L.; Lam, J.C. Changes in bioclimates in different climates around the world and implications for the built environment. *Build. Environ.* **2012**, *57*, 214–222. [CrossRef]
187. Zhou, Y.; Eom, J.; Clarke, L. The effect of global climate change, population distribution, and climate mitigation on building energy use in the U.S. and China. *Clim. Chang.* **2013**, *119*, 979–992. [CrossRef]
188. Morakinyo, T.E.; Ren, C.; Shi, Y.; Lau, K.K.L.; Tong, H.W.; Choy, C.W.; Ng, E. Estimates of the Impact of Extreme Heat Events on Cooling Energy Demand in Hong Kong. *Renew. Energy* **2019**, *142*, 73–84. [CrossRef]
189. Chan, A.L.S. Developing a modified typical meteorological year weather file for Hong Kong taking into account the urban heat island effect. *Build. Environ.* **2011**, *46*, 2434–2441. [CrossRef]
190. Zhou, Y.; Zhuang, Z.; Yang, F.; Yu, Y.; Xie, X. Urban morphology on heat island and building energy consumption. *Procedia Eng.* **2017**, *205*, 2401–2406. [CrossRef]
191. Onishi, A.; Cao, X.; Ito, T.; Shi, F.; Imura, H. Evaluating the potential for urban heat-island mitigation by greening parking lots. *Urban For. Urban Green.* **2010**, *9*, 323–332. [CrossRef]
192. Tan, Z.; Lau, K.L.; Ng, E. Urban tree design approaches for mitigating daytime urban heat island effects in a high-density urban environment. *Energy Build.* **2015**, *114*, 265–274. [CrossRef]
193. Xu, X.; Sun, S.; Liu, W.; García, E.H.; He, L.; Cai, Q.; Xu, S.; Wang, J.; Zhu, J. The cooling and energy saving effect of landscape design parameters of urban park in summer: A case of Beijing, China. *Energy Build.* **2017**, *149*, 91–100. [CrossRef]
194. Du, X.; Li, Q. The Effect of Pearl River on Summer Urban Thermal Environment of Guangzhou. *Procedia Eng.* **2017**, *205*, 1785–1791. [CrossRef]
195. Yan, H.; Wu, F.; Dong, L. Influence of a large urban park on the local urban thermal environment. *Sci. Total Environ.* **2018**, *622–623*, 882–891. [CrossRef] [PubMed]
196. Chang, C.R.; Li, M.H. Effects of urban parks on the local urban thermal environment. *Urban For. Urban Green.* **2014**, *13*, 672–681. [CrossRef]
197. Kong, F.; Sun, C.; Liu, F.; Yin, H.; Jiang, F.; Pu, Y.; Cavan, G.; Synthina, S.; Middel, A.; Dronova, I. Energy saving potential of fragmented green spaces due to their temperature regulating ecosystem services in the summer. *Appl. Energy* **2016**, *183*, 1428–1440. [CrossRef]
198. Zhang, B.; Xie, G.; Gao, J.; Yang, Y. The cooling effect of urban green spaces as a contribution to energy-saving and emission-reduction: A case study in Beijing, China. *Build. Environ.* **2014**, *76*, 37–43. [CrossRef]
199. Xiao, X.D.; Dong, L.; Yan, H.; Yang, N.; Xiong, Y. The influence of the spatial characteristics of urban green space on the urban heat island effect in Suzhou Industrial Park. *Sustain. Cities Soc.* **2018**, *40*, 428–439. [CrossRef]
200. Du, H.; Cai, Y.; Zhou, F.; Jiang, H.; Jiang, W.; Xu, Y. Urban blue-green space planning based on thermal environment simulation: A case study of Shanghai, China. *Ecol. Indic.* **2019**, *106*, 105501. [CrossRef]
201. Beni, M.A.; Zhang, B.; Xie, G.; Xu, J. Impact of urban park's tree, grass and waterbody on microclimate in hot summer days: A case study of Olympic Park in Beijing, China. *Urban For. Urban Green.* **2018**, *32*, 1–6. [CrossRef]
202. Tong, S.; Wong, N.H.; Tan, C.L.; Jusuf, S.K.; Ignatius, M.; Tan, E. Impact of urban morphology on microclimate and thermal comfort in northern China. *Solar Energy* **2017**, *155*, 212–223. [CrossRef]
203. Besir, A.B.; Cuce, E. Green roofs and facades: A comprehensive review. *Renew. Sustain. Energy Rev.* **2018**, *82*, 915–939. [CrossRef]
204. Kokogiannakis, G.; Tietje, A.; Darkwa, J. The role of Green Roofs on Reducing Heating and Cooling Loads: A Database across Chinese Climates. *Procedia Environ. Sci.* **2011**, *11*, 604–610. [CrossRef]
205. Wong, J.K.W.; Lau, S.K. From the 'urban heat island' to the 'green island'? A preliminary investigation into the potential of retrofitting green roofs in Mongkok district of Hong Kong. *Habitat Int.* **2013**, *39*, 25–35. [CrossRef]
206. Luo, H.; Huang, B.; Liu, X.; Zhang, K. Green Roof Assessment by GIS and Google Earth. *Procedia Environ. Sci.* **2011**, *10*, 2307–2313. [CrossRef]
207. Chen, C.F. Performance evaluation and development strategies for green roofs in Taiwan: A review. *Ecol. Eng.* **2013**, *52*, 51–58. [CrossRef]
208. Kokogiannakis, G.; Darkwa, J. Support for the integration of green roof constructions within Chinese building energy performance policies. *Energy* **2014**, *65*, 71–79. [CrossRef]
209. He, Y.; Yu, H.; Ozaki, A.; Dong, N.; Zheng, S. Long-term thermal performance evaluation of green roof system based on two new indexes: A case study in Shanghai area. *Build. Environ.* **2017**, *120*, 13–28. [CrossRef]

210. Tam, V.W.Y.; Wang, J.; Le, K.N. Thermal insulation and cost effectiveness of green-roof systems: An empirical study in Hong Kong. *Build. Environ.* **2016**, *110*, 46–54. [CrossRef]
211. Susca, T. Green roofs to reduce building energy use? A review on key structural factors of green roofs and their efects on urban climate. *Build. Environ.* **2019**, *162*, 106273. [CrossRef]
212. Cao, J.; Hu, S.; Dong, Q.; Liu, L.; Wang, Z. Green roof cooling contributed by plant species with different photosynthetic strategies. *Energy Build.* **2019**, *195*, 45–50. [CrossRef]
213. Peng, L.L.H.; Jim, C.Y. Economic evaluation of green-roof environmental benefits in the context of climate change: The case of Hong Kong. *Urban For. Urban Green.* **2015**, *14*, 554–561. [CrossRef]
214. Gao, Y.; Shi, D.; Levinson, R.; Guo, R.; Lin, C.; Ge, J. Thermal performance and energy savings of white and sedum-tray garden roof: A case study in a Chongqing office building. *Energy Build.* **2017**, *156*, 343–359. [CrossRef]
215. Tang, M.; Zheng, X. Experimental study of the thermal performance of an extensive green roof on sunny summer days. *Appl. Energy* **2019**, *242*, 1010–1021. [CrossRef]
216. Li, Z.; Chow, D.H.C.; Yao, J.; Zheng, X.; Zhao, W. The effectiveness of adding horizontal greening and vertical greening to courtyard areas of existing buildings in the hot summer cold winter region of China: A case study for Ningbo. *Energy Build.* **2019**, *196*, 227–239. [CrossRef]
217. He, Y.; Yu, H.; Ozaki, A.; Dong, N.; Zheng, S. Influence of plant and soil layer on energy balance and thermal performance of green roof system. *Energy* **2017**, *141*, 1285–1299. [CrossRef]
218. Zeng, C.; Bai, X.; Sun, L.; Zhang, Y.; Yuan, Y. Optimal parameters of green roofs in representative cities of four climate zones in China: A simulation study. *Energy Build.* **2017**, *150*, 118–131. [CrossRef]
219. Jiang, L.; Tang, M. Thermal analysis of extensive green roofs combined with night ventilation for space cooling. *Energy Build.* **2017**, *156*, 238–249. [CrossRef]
220. Ran, J.; Tang, M. Passive cooling of the green roofs combined with night-time ventilation and walls insulation in hot and humid regions. *Sustain. Cities Soc.* **2018**, *38*, 466–475. [CrossRef]
221. Cheng, C.Y.; Cheung, K.K.S.; Chu, L.M. Thermal performance of a vegetated cladding system on facade walls. *Build. Environ.* **2010**, *45*, 1779–1787. [CrossRef]
222. Omrany, H.; Ghaffarianhoseini, A.; Ghaffarianhoseini, A.; Raahemifar, K.; Tookey, J. Application of passive wall systems for improving the energy effciency in buildings: A comprehensive review. *Renew. Sustain. Energy Rev.* **2016**, *62*, 1252–1269. [CrossRef]
223. Safikhani, T.; Abdullah, A.M.; Ossen, D.R.; Baharvand, M. A review of energy characteristic of vertical greenery systems. *Renew. Sustain. Energy Rev.* **2014**, *40*, 450–462. [CrossRef]
224. Ling, T.Y.; Chiang, Y.C. Well-being, health and urban coherence-advancing vertical greening approach toward resilience: A design practice consideration. *J. Clean. Prod.* **2018**, *182*, 187–197. [CrossRef]
225. Zaid, S.M.; Perisamy, E.; Hussein, H.; Myeda, N.E.; Zainon, N. Vertical Greenery System in urban tropical climate and its carbon sequestration potential: A review. *Ecol. Indic.* **2018**, *91*, 57–70. [CrossRef]
226. Wong, I.; Baldwin, A.N. Investigating the potential of applying vertical green walls to high-rise residential buildings for energy-saving in sub-tropical region. *Build. Environ.* **2016**, *97*, 34–39. [CrossRef]
227. Yin, H.; Kong, F.; Middel, A.; Dronova, I.; Xu, H.; James, P. Cooling effect of direct green facades during hot summer days: An observational study in Nanjing, China using TIR and 3DPC data. *Build. Environ.* **2017**, *116*, 195–206. [CrossRef]
228. Dahanayake, K.C.; Chow, C.L.; Hou, G.L. Selection of suitable plant species for energy efficient Vertical Greenery Systems (VGS). *Energy Procedia* **2017**, *142*, 2473–2478. [CrossRef]
229. Medl, A.; Stangl, R.; Florineth, F. Vertical greening systems-A review on recent technologies and research advancement. *Build. Environ.* **2017**, *125*, 227–239. [CrossRef]
230. Seyam, S. The impact of greenery systems on building energy: Systematic review. *J. Build. Eng.* **2019**, *26*, 100887. [CrossRef]
231. Pan, L.; Chu, L.M. Energy saving potential and life cycle environmental impacts of a vertical greenery system in Hong Kong: A case study. *Build. Environ.* **2016**, *96*, 293–300. [CrossRef]
232. Zhang, L.; Deng, Z.; Liang, L.; Zhang, Y.; Meng, Q.; Wang, J.; Santamouris, M. Thermal behavior of a vertical green facade and its impact on the indoor and outdoor thermal environment. *Energy Build.* **2019**, *204*, 109502. [CrossRef]
233. Dahanayake, K.W.D.K.C.; Chow, C.L. Studying the potential of energy saving through vertical greenery systems: Using EnergyPlus simulation program. *Energy Build.* **2017**, *138*, 47–59. [CrossRef]
234. Chen, Q.; Li, B.; Liu, X. An experimental evaluation of the living wall system in hot and humid climate. *Energy Build.* **2013**, *61*, 298–307. [CrossRef]
235. He, Y.; Yu, H.; Ozaki, A.; Dong, N.; Zheng, S. An investigation on the thermal and energy performance of living wall system in Shanghai area. *Energy Build.* **2017**, *140*, 324–335. [CrossRef]
236. Li, C.; Wei, J.; Li, C. Influence of foliage thickness on thermal performance of green facades in hot and humid climate. *Energy Build.* **2019**, *199*, 72–87. [CrossRef]
237. Pan, L.; Wei, S.; Chu, L.M. Orientation effect on thermal and energy performance of vertical greenery systems. *Energy Build.* **2018**, *175*, 102–112. [CrossRef]
238. Yang, F.; Yuan, F.; Qian, F.; Zhuang, Z.; Yao, J. Summertime thermal and energy performance of a double-skin green facade: A case study in Shanghai. *Sustain. Cities Soc.* **2018**, *39*, 43–51. [CrossRef]

239. Xing, Q.; Hao, X.; Lin, Y.; Tan, H.; Yang, K. Experimental investigation on the thermal performance of a vertical greening system with green roof in wet and cold climates during winter. *Energy Build.* **2019**, *183*, 105–117. [CrossRef]
240. Zhao, C.; Fu, G.; Liu, X.; Fu, F. Urban planning indicators, morphology and climate indicators: A case study for a north-south transect of Beijing, China. *Build. Environ.* **2011**, *46*, 1174–1183. [CrossRef]
241. Zhou, X.; Chen, H. Impact of urbanization-related land use land cover changes and urban morphology changes on the urban heat island phenomenon. *Sci. Total Environ.* **2018**, *635*, 1467–1476. [CrossRef]
242. Hu, Y.; White, M.; Ding, W. An Urban Form Experiment on Urban Heat Island Effect in High Density Area. *Procedia Eng.* **2016**, *169*, 166–174. [CrossRef]
243. Liang, Z.; Wu, S.; Wang, Y.; Wei, F.; Huang, J.; Shen, J.; Li, S. The relationship between urban form and heat island intensity along the urban development gradients. *Sci. Total Environ.* **2019**, *708*, 135011. [CrossRef] [PubMed]
244. Wei, R.; Song, D.; Wong, N.H.; Martin, M. Impact of Urban Morphology Parameters on Microclimate. *Procedia Eng.* **2016**, *169*, 142–149. [CrossRef]
245. Lin, P.; Lau, S.S.Y.; Qin, H.; Gou, Z. Effects of urban planning indicators on urban heat island: A case study of pocket parks in high-rise high-density environment. *Landsc. Urban Plan.* **2017**, *168*, 48–60. [CrossRef]
246. Tong, S.; Wong, N.H.; Jusuf, S.K.; Tan, C.L.; Wong, H.F.; Ignatius, M.; Tan, E. Study on correlation between air temperature and urban morphology parameters in built environment in northern China. *Build. Environ.* **2018**, *127*, 239–249. [CrossRef]
247. Xu, D.; Zhou, D.; Wang, Y.; Xu, W.; Yang, Y. Field measurement study on the impacts of urban spatial indicators on urban climate in a Chinese basin and static-wind city. *Build. Environ.* **2018**, *147*, 482–494. [CrossRef]
248. Huang, X.; Wang, Y. Investigating the effects of 3D urban morphology on the surface urban heat island effect in urban functional zones by using high-resolution remote sensing data: A case study of Wuhan, Central China. *ISPRS J. Photogramm. Remote Sens.* **2019**, *152*, 119–131. [CrossRef]
249. Shi, Y.; Song, Z.; Zhang, W.; Song, J.; Qu, J.; Wang, Z.; Li, Y.; Xu, L.; Lin, J. Physicochemical properties of dirt-resistant cool white coatings for building energy efficiency. *Solar Energy Mater. Solar Cells* **2013**, *110*, 133–139. [CrossRef]
250. Zhang, L.; Fukuda, H.; Liu, Z. The value of cool roof as a strategy to mitigate urban heat island effect: A contingent valuation approach. *J. Clean. Prod.* **2019**, *228*, 770–777. [CrossRef]
251. Gao, Y.; Xu, J.; Yang, S.; Tang, X.; Zhou, Q.; Ge, J.; Xu, T.; Levinson, R. Cool roofs in China: Policy review, building simulations, and proof-of-concept experiments. *Energy Policy* **2014**, *74*, 190–214. [CrossRef]
252. Han, A.; Ye, M.; Liu, L.; Feng, W.; Zhao, M. Estimating thermal performance of cool coatings colored with high near-infrared reflective inorganic pigments: Iron doped La2Mo2O7 compounds. *Energy Build.* **2014**, *84*, 698–703. [CrossRef]
253. Lu, S.; Chen, Y.; Liu, S.; Kong, X. Experimental research on a novel energy efficiency roof coupled with PCM and cool materials. *Energy Build.* **2016**, *127*, 159–169. [CrossRef]
254. Qin, Y.; Liang, J.; Tan, K.; Li, F. A side by side comparison of the cooling effect of building blocks with retro-reflective and diffuse-reflective walls. *Solar Energy* **2016**, *133*, 172–179. [CrossRef]
255. Yuan, J.; Emura, K.; Farnham, C. A study on the durability of a glass bead retro-reflective material applied to building facades. *Progress Org. Coat.* **2018**, *120*, 36–48. [CrossRef]
256. Meng, X.; Luo, T.; Wang, Z.; Zhang, W.; Yan, B.; Ouyang, J. Effect of retro-reflective materials on building indoor temperature conditions and heat flow analysis for walls. *Energy Build.* **2016**, *127*, 488–498. [CrossRef]
257. Chen, J.; Wang, H.; Zhu, H. Analytical approach for evaluating temperature field of thermal modified asphalt pavement and urban heat island effect. *Appl. Therm. Eng.* **2017**, *113*, 739–748. [CrossRef]
258. Jiang, L.; Wang, L.; Wang, S. A novel solar reflective coating with functional gradient multilayer structure for cooling asphalt pavements. *Constr. Build. Mater.* **2019**, *210*, 13–21. [CrossRef]
259. Qin, Y. A review on the development of cool pavements to mitigate urban heat island effect. *Renew. Sustain. Energy Rev.* **2015**, *52*, 445–459. [CrossRef]
260. Liu, Y.; Li, T.; Peng, H. A new structure of permeable pavement for mitigating urban heat island. *Sci. Total Environ.* **2018**, *634*, 1119–1125. [CrossRef]
261. Chen, J.; Zhou, Z.; Wu, J.; Hou, S.; Liu, M. Field and laboratory measurement of albedo and heat transfer for pavement materials. *Constr. Build. Mater.* **2019**, *202*, 46–57. [CrossRef]
262. Qin, Y. Urban canyon albedo and its implication on the use of reflective cool pavements. *Energy Build.* **2015**, *96*, 86–94. [CrossRef]
263. Chen, J.; Chu, R.; Wang, H.; Zhang, L.; Chen, X.; Du, Y. Alleviating urban heat island effect using high-conductivity permeable concrete pavement. *J. Clean. Prod.* **2019**, *237*, 117722. [CrossRef]
264. Du, Y.; Han, Z.; Chen, J.; Liu, W. A novel strategy of inducing solar absorption and accelerating heat release for cooling asphalt pavement. *Solar Energy* **2018**, *159*, 125–133.
265. Jiang, W.; Xiao, J.; Yuan, D.; Lu, H.; Xu, S.; Huang, Y. Design and experiment of thermoelectric asphalt pavements with power-generation and temperature-reduction functions. *Energy Build.* **2018**, *169*, 39–47. [CrossRef]
266. Yang, L.; Qian, F.; Song, D.X.; Zheng, K.J. Research on Urban Heat-Island Effect. *Procedia Eng.* **2016**, *169*, 11–18. [CrossRef]
267. Li, A.; Deng, W.; Kong, B.; Song, M.; Feng, W.; Lu, X.; Lei, G.; Bai, J. A comparative analysis on spatial patterns and processes of three typical wetland ecosystems in 3H area, China. *Procedia Environ. Sci.* **2010**, *2*, 315–332. [CrossRef]
268. Syafii, N.I.; Ichinose, M.; Kumakura, E.; Jusuf, S.K.; Chigusa, K.; Wong, N.H. Thermal environment assessment around bodies of water in urban canyons: A scale model study. *Sustain. Cities Soc.* **2017**, *34*, 79–89. [CrossRef]

269. Cheng, L.; Guan, D.; Zhou, L.; Zhao, Z.; Zhou, J. Urban cooling island effect of main river on a landscape scale in Chongqing, China. *Sustain. Cities Soc.* **2019**, *47*, 101501. [CrossRef]
270. Wang, C.; Zhu, W. Analysis of the Impact of Urban Wetland on Urban Temperature Based on Remote Sensing Technology. *Procedia Environ. Sci.* **2011**, *10*, 1546–1552.
271. Xue, Z.; Hou, G.; Zhang, Z.; Lyu, X.; Jiang, M.; Zou, Y.; Shen, X.; Wang, J.; Liu, X. Quantifying the cooling-effects of urban and peri-urban wetlands using remote sensing data: Case study of cities of Northeast China. *Landsc. Urban Plan.* **2019**, *182*, 92–100. [CrossRef]
272. Xu, X.; Liu, S.; Sun, S.; Zhang, W.; Liu, Y.; Lao, Z.; Guo, G.; Smith, K.; Cui, Y.; Liu, W.; et al. Evaluation of Energy Saving Potential of an Urban Green Space and its Water Bodies. *Energy Build.* **2019**, *2019*, 58–70. [CrossRef]
273. Sun, R.; Chen, L. How can urban water bodies be designed for climate adaptation? *Landsc. Urban Plan.* **2012**, *105*, 27–33. [CrossRef]
274. Wu, C.; Li, J.; Wang, C.; Song, C.; Song, C.; Chen, Y.; Finka, M.; Rosa, D.L. Understanding the relationship between urban blue infrastructure and land surface temperature. *Sci. Total Environ.* **2019**, *694*, 133742. [CrossRef] [PubMed]
275. Cai, Z.; Han, G.; Chen, M. Do water bodies play an important role in the relationship between urban form and land surface temperature? *Sustain. Cities Soc.* **2018**, *39*, 487–498. [CrossRef]
276. Wu, D.; Wang, Y.; Fan, C.; Xia, B. Thermal environment effects and interactions of reservoirs and forests as urban blue-green infrastructures. *Ecol. Indic.* **2018**, *91*, 657–663. [CrossRef]
277. Hsieh, C.M.; Huang, H.C. Mitigating urban heat islands: A method to identify potential wind corridor for cooling and ventilation. *Comput. Environ. Urban Syst.* **2016**, *57*, 130–143. [CrossRef]
278. Su, N.; Zhou, D.; Jiang, X. Study on the Application of Ventilation Corridor Planning in Urban New Area-A Case Study of Xixian New Area. *Procedia Eng.* **2016**, *169*, 340–349. [CrossRef]
279. Yang, L.; Li, Y. Thermal conditions and ventilation in an ideal city model of Hong Kong. *Energy Build.* **2011**, *43*, 1139–1148. [CrossRef]
280. Luo, Y.; He, J.; Ni, Y. Analysis of urban ventilation potential using rule-based modeling. *Comput. Environ. Urban Syst.* **2017**, *66*, 13–22. [CrossRef]
281. Ren, C.; Yang, R.; Cheng, C.; Xing, P.; Fang, X.; Zhang, S.; Wang, H.; Shi, Y.; Zhang, X.; Kwok, Y.T.; et al. Creating breathing cities by adopting urban ventilation assessment and wind corridor plan-The implementation in Chinese cities. *J. Wind Eng. Ind. Aerodyn.* **2018**, *182*, 170–188. [CrossRef]
282. Xu, D.; Zhou, D. Research on the Planning Methods of Mitigating Summer Urban Heat Island Effects among Basin Cities—A Case Study at Xi'an, China. *Procedia Eng.* **2016**, *169*, 248–255. [CrossRef]
283. Guo, F.; Zhu, P.; Wang, S.; Duan, D.; Jin, Y. Improving Natural Ventilation Performance in a High-Density Urban District: A Building Morphology Method. *Procedia Eng.* **2017**, *205*, 952–958. [CrossRef]
284. Wang, W.; Ng, E.; Yuan, C.; Raasch, S. Large-eddy simulations of ventilation for thermal comfort-A parametric study of generic urban configurations with perpendicular approaching winds. *Urban Clim.* **2017**, *20*, 202–227. [CrossRef]
285. Qiao, Z.; Xu, X.; Wu, F.; Luo, W.; Wang, F.; Liu, L.; Sun, Z. Urban ventilation network model: A case study of the core zone of capital function in Beijing metropolitan area. *J. Clean. Prod.* **2017**, *168*, 526–535. [CrossRef]
286. Wu, Z.; Chen, R.; Meadows, M.E.; Sengupta, D.; Xu, D. Changing urban green spaces in Shanghai: Trends, drivers and policy implications. *Land Use Policy* **2019**, *87*, 104080. [CrossRef]
287. Morakinyo, T.E.; Lai, A.; Lau, K.K.L.; Ng, E. Thermal benefits of vertical greening in a high-density city: Case study of Hong Kong. *Urban For. Urban Green.* **2019**, *37*, 42–55. [CrossRef]